
DPZV: Elevating the Tradeoff between Privacy and Utility in Zeroth-Order Vertical Federated Learning

Jianing Zhang Evan Chen Chaoyue Liu Christopher G. Brinton
Elmore Family School of Electrical and Computer Engineering
Purdue University
West Lafayette, IN 47907
{zhan4670, chen4388, cyliu, cgb}@purdue.edu

Abstract

Vertical Federated Learning (VFL) enables collaborative training with feature-partitioned data, yet remains vulnerable to privacy leakage through gradient transmissions. Standard differential privacy (DP) techniques like DP-SGD are difficult to apply in this setting due to VFL’s distributed nature and the high variance incurred by vector-valued noise. On the other hand, zeroth-order (ZO) optimization techniques can avoid explicit gradient exposure, but lack formal privacy guarantees. In this work, we propose DPZV, the first ZO optimization framework for VFL that achieves tunable DP with performance guarantees. DPZV overcomes the aforementioned limitations by injecting low-variance scalar noise at the server, enabling controllable privacy with reduced memory overhead. We conduct a comprehensive theoretical analysis showing that DPZV matches the convergence rate of first order (FO) optimization methods while satisfying formal (ϵ, δ) -DP guarantees. Experiments on image and language benchmarks demonstrate that DPZV outperforms several baselines in terms of achieved accuracy under a wide range of privacy constraints ($\epsilon \leq 10$), thereby elevating the privacy-utility tradeoff in VFL.

1 Introduction

Vertical Federated Learning (VFL) has emerged as a compelling paradigm for training models on data that are partitioned feature-wise among distinct parties [3, 4, 15]. It seeks to preserve privacy by maintaining separate submodels locally and exchanging only intermediate representations or gradients, without exposing their raw data. Despite its privacy-aware architecture, recent studies have demonstrated that VFL remains vulnerable to feature leakage [19, 36] and label leakage [13, 41], where adversaries can infer sensitive input attribute or labels from the exchanged model updates or intermediate gradients. These findings highlight a critical need for integrating stronger, principled privacy-preserving mechanisms into the VFL framework.

One direction for mitigating privacy risks in VFL is through replacing SGD-based updates with zeroth-order (ZO) optimization [28]. By avoiding the transmission of intermediate gradients, ZO naturally reduces the risk of label leakage [39]. However, the privacy level of ZO-based methods are not directly adjustable, which constrains their applicability in settings that demand adaptive privacy guarantees aligned with task-specific requirements. Moreover, ZO remains susceptible to feature leakage, since sensitive information may still be inferred from local model parameters.

Importantly, current ZO-based VFL algorithms fail to provide mathematically rigorous differential privacy (DP) [10] guarantees, unlike their SGD counterparts. The DP mechanism is desirable as it allows for adjustable privacy levels under varying privacy budgets, enabling flexible trade-offs

between model performance and privacy [11]. It also offers protection against a broad class of inference attacks [22, 31, 40]. As a result, in this work, we ask the following research question:

How can we incorporate a controllable differential privacy mechanism into zeroth-order VFL which maintains convergence guarantees while elevating the privacy-utility tradeoff?

Key Challenges. Integrating differential privacy into ZO-based VFL poses several fundamental challenges. In particular, existing strategies for achieving DP within the VFL framework typically involve injecting vector-valued noise into either (i) forward embeddings or (ii) backward gradients [4, 35]. While approach (i) can provide formal privacy guarantees, it requires adding noise with the same shape as the transmitted embeddings, which are typically high-dimensional. This high-dimensional noise introduces substantial variance amplification [1]. Moreover, ZO methods inherently produce noisy gradient estimates [14]: when combined with the additional variance introduced by DP noise, the compounded effect can lead to substantial performance degradation. This situation can be further exacerbated when the privacy budget is tight. On the other hand, approach (ii) is incompatible with ZO methods, as ZO does not involve transmitting backward gradients [12].

Contributions. To address the above challenges, we propose Differentially Private Zeroth-Order VFL (DPZV), a novel ZO-based VFL framework that achieves a controllable differential privacy level with convergence guarantees. By injecting *scalar-valued* noise rather than high-dimensional vector noise, DPZV mitigates variance amplification, thereby enhancing the tradeoff between privacy and model performance in VFL. Our main contributions can be summarized as follows:

- DPZV is the first ZO optimization framework for vertical federated learning (VFL) that enables tunable differential privacy. By injecting calibrated scalar-valued noise instead of high-dimensional vector noise, DPZV provides privacy guarantees while preserving model accuracy. Moreover, the use of ZO optimization substantially reduces memory overhead, making DPZV particularly suitable for privacy-critical and resource-constrained environments (Sec. 4).
- We provide a rigorous theoretical analysis establishing both convergence and privacy guarantees for DPZV. Specifically, we show that DPZV achieves a convergence rate on the same order as first-order DP-SGD, despite using only ZO estimators. This result indicates that our DPZV framework attains privacy without sacrificing training efficiency. Furthermore, we prove that our method satisfies (ϵ, δ) -DP, confirming its ability to provide an adjustable privacy control mechanism (Sec. 5 and 6).
- Through experiments on image and language benchmarks, we demonstrate that DPZV obtains robust convergence performance under strict privacy budgets. While other DP baselines experience a steep performance degradation as the privacy level increases, DPZV consistently maintains high accuracy across all tasks, underscoring an elevated tradeoff between privacy and utility (Sec. 7).

2 Related Work

Vertical Federated Learning. Vertical Federated Learning (VFL) enables collaborative training across organizations with vertically partitioned features. Early VFL frameworks focused on simple client-side models such as logistic regression and linear models [15], where clients computed local gradients for global aggregation. These methods prioritized simplicity, but lacked expressiveness for complex tasks. To address this limitation, larger client-side models like deep neural networks (DNNs) were adopted [3, 4, 35]. Studies have demonstrated that these larger client-side models can be more effective than classical methods [23]. However, larger models require higher processing capability and VRAM costs, which calls for computation and memory efficient methods.

In an effort to reduce communication cost, several communication-efficient VFL methods have been proposed. One popular mechanism for reducing communication overhead is by allowing for multiple local updates in-between aggregations. In this respect, [24] introduced FedBCD, a federated stochastic block coordinate descent method, which allows clients to perform multiple gradient iterations before synchronization. Similarly, Flex-VFL [3] proposed a flexible strategy offering varying local update counts per party, constrained by a communication timeout. VIMADMM [35] adopted an ADMM-based approach to enable multiple local updates in VFL. All these methods effectively reduce the number of round-trip communications in each iteration. On the other hand, Asynchronous VFL methods (e.g., FDML [17], VAFL [4]) decouple coordination, allowing clients to update models independently. While asynchronous methods risk staleness, they significantly improve scalability in cross-silo deployments. However, in first-order methods, the backward pass through neural networks typically imposes

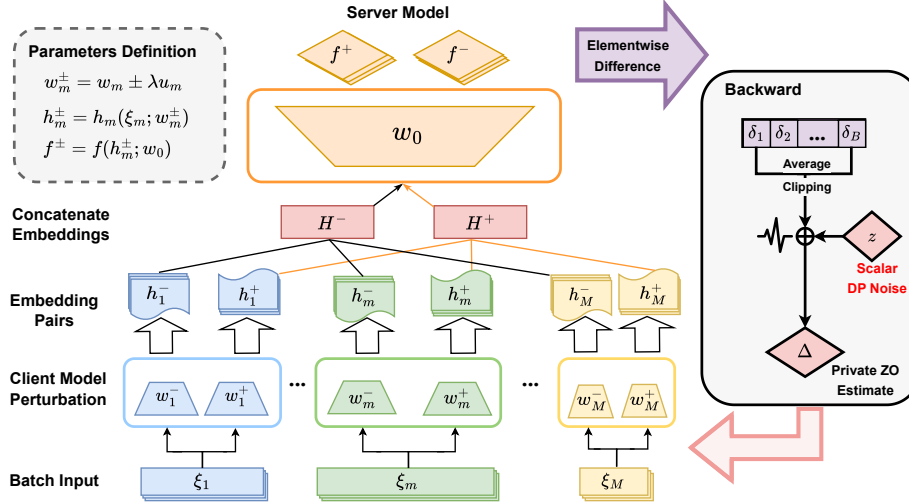


Figure 1: Overview of the training procedure in DPZV. Each client perturbs its local model parameters in two random directions to generate a pair of embeddings, which are then transmitted to the server. The server computes the corresponding function evaluations and applies an elementwise difference to approximate the zeroth-order (ZO) gradient. To ensure differential privacy, scalar-valued Gaussian noise is injected into the aggregated ZO estimate. Unlike traditional vector-valued noise in standard DP algorithms, scalar noise is significantly smaller in norm, thereby preserving model utility even under stringent privacy budgets.

communication overhead comparable to the forward pass. In contrast, our ZO-based approach significantly reduces the cost associated with backward propagation.

Privacy guarantees are critical for VFL adoption. Some VFL architectures use crypto-based privacy-preserving techniques such as Homomorphic Encryption (HE) [6], but lack formal assurances, while DP provides rigorous mathematical protection. Key DP-based methods include VAFL [4], which injects Gaussian noise into client embeddings during forward propagation to achieve Gaussian DP, and VIMADMM [35], which perturbs linear model parameters with bounded sensitivity, ensuring DP guarantees for convex settings. Our work overcomes challenges in developing such methods for the ZO setting.

Zeroth-Order Optimization. Recent research has explored Zeroth-Order (ZO) optimization within VFL to accommodate resource-constrained clients with non-differentiable models and to reduce gradient leakage. Early work like ZOO-VFL [39] adopted a naive ZO approach throughout VFL training but provided no DP guarantees. VFL-CZOF0 [33] introduced a cascaded hybrid optimization method, combining zeroth-order and first-order updates, which leveraged intrinsic noise from ZO for limited privacy. However, its DP level was not adjustable, often resulting in insufficient protection.

More recently, MeZO [26] proposed a memory-efficient ZO algorithm. Building upon these ideas, DPZero [38] and DPZO [32] introduced private ZO variants offering baseline privacy features. However, these methods are designed for centralized settings and cannot be directly extended to the VFL paradigm. In this work, we incorporate the memory-efficient design of MeZO into a VFL framework. Extending beyond previous efforts to combine ZO optimization with VFL, we further integrate a controllable differential privacy mechanism, achieving an elevated trade-off between privacy and model performance.

3 Background and Motivation

System Model for VFL. We consider a VFL framework with one server and M clients. In VFL, data is vertically partitioned between clients, with each client holding different features of the data. Suppose we have a dataset \mathcal{D} with D samples: $\mathcal{D} = \{\xi_i | i = 1, 2, \dots, D\}$. Each data sample ξ_i can be partitioned into M portions distributed throughout all clients, where the data sample on machine m with ID i is denoted as $\xi_{m,i}$, hence $\xi_i = [\xi_{1,i}, \xi_{2,i}, \dots, \xi_{M,i}]^\top$. The server is numbered as machine 0 and holds the label data $\mathbf{Y} = \{y_i | i = 1, 2, \dots, D\}$.

The clients and the server aim to jointly train a machine learning model parameterized by w . The global model comprises local models on each party parameterized by w_m , with $m = 0, 1, \dots, M$ being the ID of the machine. To protect privacy, clients do not communicate with each other regarding data or model parameters. Instead, all clients communicate directly with the server regarding their local model’s outputs, which we term as local embeddings. If we denote the local embedding of client m as $h_{m,i} := h(w_m; \xi_{m,i})$, the objective of the VFL framework can be seen as minimizing the following function:

$$F(w; \mathcal{D}, \mathbf{Y}) := \frac{1}{D} \sum_{i \in [D]} \mathcal{L}(w_0, h_{1,i}, h_{2,i}, \dots, h_{M,i}; y_i) \quad (1)$$

where \mathcal{L} is the loss function for a datum ξ_i and its corresponding label y_i . For the simplicity of notation, we define the loss function w.r.t a specific model parameter and datum as

$$f(w; \xi_i) := \mathcal{L}(w_0, h_{1,i}, h_{2,i}, \dots, h_{M,i}; y_i) \quad (2)$$

Memory-Efficient Zeroth-Order Optimizer. We introduce the two-point gradient estimator [30], which will serve as our zeroth-order gradient estimator throughout this paper. Let u be uniformly sampled from the Euclidean sphere $\sqrt{d}\mathbb{S}^{d-1}$ and $\lambda > 0$ be the smoothing factor. For a single datum ξ sampled from the whole dataset \mathcal{D} , the two-point gradient estimator is defined as

$$g(x; \xi) = \frac{f(x+\lambda u; \xi) - f(x-\lambda u; \xi)}{2\lambda} u \quad (3)$$

To further reduce the memory overhead on client, we adopt the MeZO methodology [26] for our ZO Optimization, which requires only the same memory as the model itself for training. We investigate the memory reduction in Appendix F.

Differential Privacy and DP-SGD. Differential Privacy (DP) provides a principled framework for protecting individual data in statistical analysis and machine learning. Formally, we adopt the standard (ϵ, δ) -DP definition:

Definition 3.1 ((ϵ, δ) -Differential Privacy). A randomized algorithm $\mathcal{M} : \mathcal{X}^n \rightarrow \Theta$ is said to satisfy (ϵ, δ) -differential privacy if for any neighboring datasets $X, X' \in \mathcal{X}^n$ that differ by only one individual’s data, and for any subset of outputs $E \subseteq \Theta$, we have

$$\mathbb{P}[\mathcal{M}(X) \in E] \leq e^\epsilon \mathbb{P}[\mathcal{M}(X') \in E] + \delta. \quad (4)$$

One of the most widely adopted private training algorithms is Differentially Private Stochastic Gradient Descent (DP-SGD), which operates by clipping an intermediate result and injecting Gaussian noise during each model update. Specifically, given a minibatch B_t at iteration t , DP-SGD performs the following steps: 1) Clip individual gradients: $\bar{g}_i = \nabla \ell(\theta_t, x_i)$, $\tilde{g}_i = \bar{g}_i / \max\left(1, \frac{\|\bar{g}_i\|_2}{C}\right)$. 2) Add Gaussian noise: $\tilde{g}_t = \frac{1}{|B_t|} \left(\sum_{i \in B_t} \tilde{g}_i + \mathcal{N}(0, \sigma^2 C^2 \mathbf{I})\right)$. 3) Update model: $\theta_{t+1} = \theta_t - \eta_t \tilde{g}_t$.

Challenges and Motivation. While DP-SGD is effective in centralized or horizontally federated setups, it becomes more challenging in VFL, particularly when ZO optimization is employed. First, *due to the distributed nature of VFL, differential privacy must be enforced before the server communicates with clients to protect against potential inference attacks by malicious client parties.* In both cases, the noise must match the dimensionality of the protected vector (embedding or gradient), often resulting in high-dimensional noise. This situation is further exacerbated by the second factor: in ZO methods, gradients are approximated through multiple forward evaluations, making them inherently noisy. Adding a *high-dimensional* noise vector as in standard DP-SGD further amplifies this inaccuracy.

A notable benefit of ZO optimization is its communication efficiency in the backward pass, where only a scalar value instead of high-dimensional gradients are transmitted. This enables *a more efficient privacy mechanism—injecting scalar noise rather than high-dimensional noise.* Motivated by this observation, we develop Differentially Private Zeroth-Order Vertical Federated Learning (DPZV), a framework that achieves tunable differential privacy through calibrated scalar noise injection. This design allows for a favorable privacy-utility trade-off in ZO-based VFL, particularly under tight privacy budgets.

4 Methodology

In this section, we describe the overall training procedure of DPZV. Based on (1), the objective is to collaboratively minimizing global objective function across all clients, each holds disjoint features

Algorithm 1: DPZV: Differentially Private Zeroth-Order Vertical Federated Learning

Input : Data \mathcal{D} , batch size B , learning rate η_m , total iteration T , smoothing parameter $\lambda_m > 0$, clipping threshold $C > 0$, privacy parameter σ_{dp}

Output : Parameter w_0, w_m for all parties $m \in [M]$

- 1 Initialize w_0, w_m and set $t, t_m = 0$ for all parties
 - 2 **for** $t = 1, \dots, T$ **do**
 - 3 Sample ready-to-update client $m \in \{1, \dots, M\}$.
 - 4 Client m samples a mini-batch $\mathcal{B}_m^{t_m}$ with corresponding IDs $\mathcal{I}_m^{t_m}$.
 - 5 Client m computes perturbed local embeddings $\{h_{m,i}^{t_m^+}, h_{m,i}^{t_m^-}\}_{i \in \mathcal{I}_m^{t_m}}$ according to (6).
 - 6 **(Forward)** Client transmits embeddings to server.
 - 7 Server computes Δ_m^t according to (7) and (8), and updates via ZO Optimization.
 - 8 **(Backward)** Client receives Δ_m^t .
 - 9 Client performs local update using (9).
 - 10 Client update local time stamp $t_m = t$.
-

of the same data records, and one server which holds the label data. The training procedure can be described in two iterative steps: (i) *Client Update and Forward Communication*: The sampled client computes local information and transmits it to the server, we define the client-server communication as *forward communication*. (ii) *Server Update and Backward Communication*: The server updates the global model and transmit global updates to the client, we define the server-client communication as *backward communication*.

Training Procedure. Each client m maintaining its own local communication round t_m , while the server tracks a global round t . Whenever the server receives information from a client, it increments t . Upon receiving an update from the server, the client synchronizes by setting $t_m = t$, capturing the latest state. This asynchronous mechanism allows clients to progress without waiting for stragglers, improving throughput and minimizing idle time. The server maintains a copy of the latest local embeddings $\tilde{h}_{m,i}^t$ for all clients $m \in [M]$ and data samples $\xi_i \in \mathcal{D}$. Due to the asynchronous nature of the algorithm, these copies may be stale, as they do not always reflect the most up-to-date model parameters of the clients. Let $\tilde{t}_{m,i}$ denote the client time when the server last updated $\tilde{h}_{m,i}^t$. The delay at server communication round t can then be expressed as $\tau_m^t = t_m - \tilde{t}_{m,i}$, where the delayed model parameters are defined as:

$$\tilde{\chi}^t = \{w_1^{t_1 - \tau_1^t}, \dots, w_M^{t_M - \tau_M^t}\}, \quad \tilde{w}^t = \{w_0^t, \tilde{\chi}^t\}. \quad (5)$$

Local Embedding Perturbation. For each global iteration t , a client m is activated, and it samples a mini-batch $\mathcal{B}_m^{t_m} \in \mathcal{D}$ and the corresponding IDs $\mathcal{I}_m^{t_m}$. To approximate gradients via zeroth-order finite differences, client m computes two perturbed local embeddings for the mini-batch,

$$\begin{aligned} \{h_{m,i}^{t_m^+}\}_{i \in \mathcal{I}_m^{t_m}} &= \{h(w_m^{t_m} + \lambda_m \mathbf{u}_m^{t_m}; \xi_{m,i})\}_{i \in \mathcal{I}_m^{t_m}}, \\ \{h_{m,i}^{t_m^-}\}_{i \in \mathcal{I}_m^{t_m}} &= \{h(w_m^{t_m} - \lambda_m \mathbf{u}_m^{t_m}; \xi_{m,i})\}_{i \in \mathcal{I}_m^{t_m}} \end{aligned} \quad (6)$$

where $\mathbf{u}_m^{t_m}$ is sampled uniformly at random from the Euclidean sphere $\sqrt{d_m} \mathbb{S}^{d_m-1}$, and λ_m is a smoothing parameter that controls the step size of perturbation. These two perturbed embeddings serve as “positive” and “negative” perturbations of its local parameters, which are forwarded to the server for further computation.

Server Side ZO Computation. After the server receives the local embeddings $h_{m,i}^{t_m}$ from client m , it updates its embeddings copy and do computation. For each embedding pair $\{h_{m,i}^{t_m^+}, h_{m,i}^{t_m^-}\}$, it computes the difference in loss function \mathcal{L} caused by perturbation, divided by the smooth parameter λ_m . Specifically, we define¹:

$$\delta_{m,i}^{t,t_m} = \frac{\tilde{f}(w_0, h_{m,i}^{t_m^+}; y_i) - \tilde{f}(w_0, h_{m,i}^{t_m^-}; y_i)}{\lambda_m}, \quad (7)$$

¹We slightly abuse the notation, and define $\tilde{f}(w_0, h_{m,i}^{t_m^\pm}; y_i) = \mathcal{L}(w_0, \tilde{h}_{1,i}^t, \dots, h_{m,i}^{t_m^\pm}, \dots, \tilde{h}_{M,i}^t; y_i)$. where we treat \tilde{f} as a function of the server parameter w_0 and the perturbed local embeddings.

Scalar DP Noise Injection. To ensure controllable privacy, the server then clips each $\delta_{m,i}^t$ by a threshold C to bound sensitivity: $\text{clip}_C(\delta_{m,i}^t) = \min\{\delta_{m,i}^t, C\}$. It then samples noise z_m^t from a Gaussian distribution $\mathcal{N}(0, \sigma_{dp}^2)$. This noise is added to the mean of the per-sample-clipped updates, yielding a differentially private gradient-like quantity:

$$\Delta_m^t = \frac{1}{B} \sum_{i \in \mathcal{I}_m^t} \text{clip}_C(\delta_{m,i}^t) + z_m^t. \quad (8)$$

The server then performs a backward communication and sends Δ_m^t to client m . The server then updates its global model through two possible operations: *i*) ZO Optimization, $\mathbf{w}_0 \leftarrow \mathbf{w}_0 - \eta_0 g(\mathbf{w}_0; \xi_i)$ (defined in (3)); or *ii*) stochastic gradient descent (SGD), $\mathbf{w}_0 \leftarrow \mathbf{w}_0 - \eta_0 \nabla_{\mathbf{w}_0} F(\mathbf{w}; \xi_i)$, depending on the constraints on computation resources. The adopted ZO update methodology is explained in Section 3. On the client side, upon receiving Δ_m^t , client m updates its local parameter \mathbf{w}_m with learning rate η_m :

$$\mathbf{w}_m \leftarrow \mathbf{w}_m - \eta_m \Delta_m^t \mathbf{u}_m^{t_m}, \quad (9)$$

where $\mathbf{u}_m^{t_m}$ is the same vector used for local perturbation. Our method is well-suited for resource-constrained environments, such as edge devices with limited VRAM or computation power, while still maintaining robust performance and scalability in VFL settings. We summarize the pipeline above in Algorithm 1.

5 Convergence Analysis

In this section, we provide the convergence analysis for DPZV. The detailed proofs can be found in Appendix B. For brevity, we define the following notations: $F^t = F(\mathbf{w}^t) := F(\mathbf{w}^t; \mathcal{D}, \mathbf{Y})$, and $f(\mathbf{w}; \xi_i)$ as defined in (2). We make the following standard assumptions²:

Assumption 5.1 (Properties of loss function). The VFL objective function F is bounded from below, the function $f(\mathbf{w}; \xi_i)$ is ℓ -Lipschitz continuous and L -Smooth for every $\xi_i \in \mathcal{D}$.

Assumption 5.2 (System boundedness). The following system dynamics are bounded: 1) *Stochastic Noise*: The variance of the stochastic first order gradient is upper bounded in expectation: $\mathbb{E} \left[\|\nabla_{\mathbf{w}} f(\mathbf{w}; \xi) - \nabla_{\mathbf{w}} F(\mathbf{w})\|^2 \right] \leq \sigma_s^2$. 2) *Time Delay*: The parameter delay τ_m^t is upper bounded by a constant τ : $\tau^t \leq \tau, \quad \forall m, t$.

Assumption 5.3 (Independent Participation). Under an asynchronous update system, the probability of one client participating in one communication round is independent of other clients and satisfies: $\mathbb{P}(\text{client } m \text{ uploading}) = q_m$.

We now present the main theorem that provides convergence guarantee for DPZV:

Theorem 5.4. *Under Theorem 5.1-5.3. Define $\mathcal{F} = \mathbb{E}[F^0 - F^T]$. If we denote $q_* = \min_m q_m$, $d_* = \max_m d_m$ where d_m represent the dimension of model parameters on device m , and let all step sizes satisfy: $\eta_0 = \eta_m = \eta \leq \min\left\{\frac{1}{\sqrt{T}d_*}, \frac{B}{4L(B+8d_0)+8\gamma_1(2d_m+B)}\right\}$, let the smoothing parameter λ*

satisfy: $\lambda \leq \frac{1}{Ld\sqrt{T}}$, and let the clipping level C satisfy: $C \geq \max\left\{0, \frac{1}{2}L\lambda d - \ell\sqrt{8\log(2\sqrt{2\pi})}\right\}$,

then for any given global iteration $T \geq 1$, we have the following upper bound on the gradient norm:

$$\frac{1}{T} \sum_{t=0}^{T-1} \mathbb{E} \left[\|\nabla_{\mathbf{w}} F(\mathbf{w}^t)\|^2 \right] \leq \mathcal{O} \left(\frac{\mathcal{F}\sqrt{d_*}}{\sqrt{T}} + \frac{d_*}{T} + \frac{(\sigma_s^2/B + \sigma_{dp}^2)\sqrt{d_*}}{\sqrt{T}} + \frac{C^2\sqrt{d_*}}{(\exp(C^2)-1)B\sqrt{T}} \right), \quad (10)$$

Discussion. The first term is influenced by the model's initialization, F^0 . This term also enjoys the same rate as ZO optimization in the centralized case [14]. The second term $\mathcal{O}(\frac{d_*}{T})$ is a standard term for ZOO methods based on the usage of ZO estimator updates. The third term captures the impact of various noise sources in the learning system. Here, σ_s^2/B represents the noise introduced by stochastic gradients, and σ_{dp}^2 corresponds to the variance of the injected DP noise. While reducing σ_{dp}^2 improves utility, it comes at the cost of weakening privacy guarantees. Consequently, this term

²We claim that Theorem 5.1 and 5.2 are standard in VFL and ZO literature [3, 33]. We follow [38] to make the ℓ -Lipschitz assumption in order to bound the probability of clipping. Theorem 5.3 is common when dealing with asynchronous participation [4], and can be satisfied when the activations of clients follow independent Poisson processes.

encapsulates the fundamental trade-off between model performance, computational cost, and privacy budget. The fourth term, quantifies the impact of the gradient clipping operation on convergence. As C increases, this term diminishes, effectively recovering the non-private case in the limit. However, the noise variance σ_{dp}^2 also scales linearly with C , which can impede overall convergence. This trade-off underscores the importance of carefully tuning the sensitivity level to balance privacy preservation and learning efficiency.

Based on the privacy analysis in Section 6, we further substitute the level of DP variance $\sigma_{dp} = \frac{2C\sqrt{T}}{D\mu}$ into this convergence rate. By selecting $T = \mathcal{O}\left(\frac{D^2\mu^2\sqrt{d}}{C^2}\left(\mathcal{F} + \frac{\sigma^2}{B} + \frac{C^2}{e^{C^2-1}}\right)\right)$, the overall convergence upper bound becomes $\mathcal{O}\left(\frac{\sqrt{d}}{D\mu}\right)$, which matches the known rate of DP-SGD for *first-order* methods [5]. This result underscores a key insight of our analysis: although zeroth-order optimization typically converges more slowly than its first-order counterpart in non-private settings, it can achieve the same convergence rate when subject to differential privacy constraints.

6 Privacy Analysis

While data are kept local in the VFL framework, the communication of local embeddings and backward gradient during the training process, as well as the sharing of model weights post training, can pose threat to sensitive information such as label and features [29]. In this section, we talk about how our algorithm protect privacy under these threat models. We consider two scenarios: 1) *Honest-but-curious*: In the honest-but-curious threat model, participants adhere strictly to the protocols of VFL without deviating from agreed procedures. However, they may attempt to infer private information from intermediate results exchanged during training. 2) *Post-training adversarial*: This model focuses on attacks conducted after the training process. It assumes the attacker lacks access to intermediate results. The adversary only has access to the trained model and aims to infer sensitive information by analyzing the model’s behavior or responses.

Theorem 6.1. *Under Theorem 5.1-5.3, suppose the privacy parameter σ_{dp} is $\sigma_{dp} = \frac{2C\sqrt{T}}{D\mu}$, where D denotes the volume of the dataset, T defines total iterations, and $\mu > 0$ controls the privacy level. The training process of Algorithm 1 is seen to be $(\epsilon, \delta(\epsilon))$ -differential private for $\forall \epsilon > 0$, where*

$$\delta(\epsilon) = \Phi\left(-\frac{\epsilon}{\mu} + \frac{\mu}{2}\right) - e^\epsilon \Phi\left(-\frac{\epsilon}{\mu} - \frac{\mu}{2}\right) \quad (11)$$

Discussion. The theorem provides privacy guarantee under the "honest-but-curious" threat model, where one or a few malicious clients try to do inference attacks by collecting information of the system. By providing only the differentially private ZO information Δ_m^t , the algorithm protects for both label inference attacks [13] and feature inference attacks [25], because the attacker cannot differentiate a single datum in the dataset \mathcal{D} and label set \mathbf{Y} . The differential privacy parameter μ is related to (ϵ, δ) through the relationship defined in (11). Given any two of these parameters, the third can be determined by solving (11), allowing full flexibility in controlling the privacy level.

Although the forward embeddings $h_{m,i}$ are not protected by differential privacy and may be vulnerable to feature attacks from the server, existing attacks primarily rely on access to model parameters w_m for model inversion [16, 18] or require backward gradients for gradient inversion [19]. Both attack vectors are mitigated under our differential privacy guarantees. A detailed discussion of our framework’s robustness against various attacks is provided in Appendix E, and the detailed proofs can be found in Appendix C.

7 Experiments

Setup. We consider four datasets: image dataset MNIST [7], CIFAR-10 [20], semantic dataset Amazon Review Polarity [27], and multi-view dataset ModelNet40 [34]. For each dataset, we conduct a grid search on learning rates and other hyperparameters. We run 100 epochs on each method and select the best validation model. We run each algorithm under three random seeds and compute the sample variance for the generosity of our result. For MNIST, we use a two-layer CNN model, for VFL’s data partitioning, we split the images by row evenly into 7 sub-images and assign them to 7 clients. For CIFAR-10 we use a four-layer CNN model, and partition each image into 2x2, 4 patches of the same size for 4 clients. For ModelNet40, we use a ResNet-18 model, and partition each object into 12 different camera views and allocate them to 12 clients. For Amazon Reviews, we

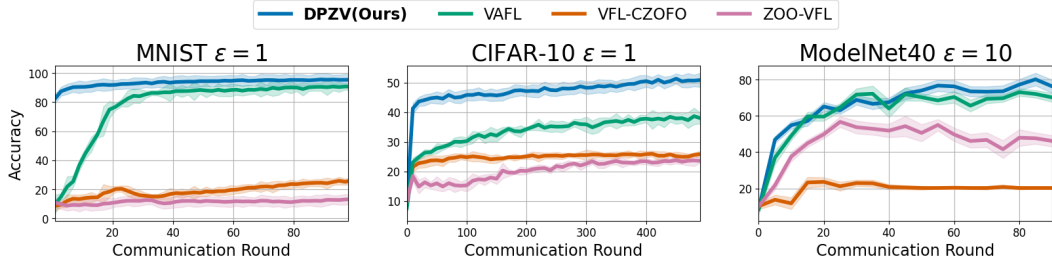


Figure 2: Test Accuracy of VFL Methods on image classification tasks under DP constraints. δ is set to 1×10^{-3} . DPZV outperforms first-order VFL methods on two datasets and surpasses all other ZO-based methods across all three datasets, showing both a higher accuracy and a faster convergence rate.

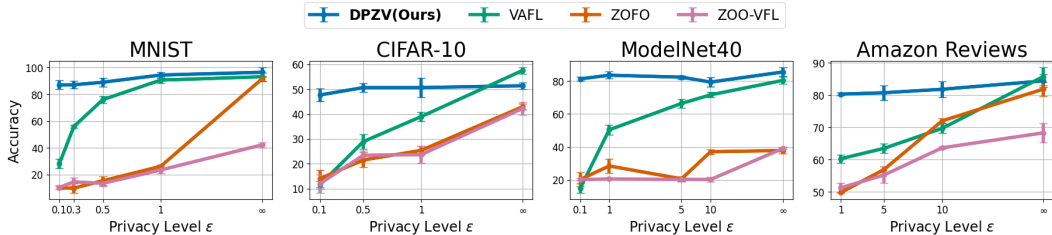


Figure 3: Privacy-Accuracy tradeoff across different datasets and algorithms. We use a constant level of $\delta = 1 \times 10^{-3}$ and vary ϵ to simulate different privacy levels. Our algorithm consistently outperforms baselines under tight privacy budget, showing a slower decay in performance than baselines as ϵ decreases.

use a pre-trained BERT [8] model, and split the tokenized data input into 3 paragraphs of the same number of tokens and distributed them across 3 clients. For all four datasets, we use a fully connected model of two linear layers with ReLU activations as the server model.

We compare our algorithm against several SotA VFL methods: 1) VAFL [4] 2) ZOO-VFL [39], 3) VFL-CZOFO [33]. All methods assume that the server holds the labels, and concatenates the embeddings of clients as the input of the server. VAFL updates its model through first-order optimization in an asynchronous manner, and achieves DP by adding random noise to the output of each local embedding. We use VAFL as a first-order baseline of VFL method. Contrary to VAFL, ZOO-VFL and ZOFO both adopt ZO optimization in their training procedure. ZOO-VFL substitutes the first order optimization by ZO optimization in common VFL methods. VFL-CZOFO uses a cascade hybrid optimization method that computes the intermediate gradient via ZOO, while keeping the back propagation on both server and client. To enforce DP and compare all methods fairly, we follow the approach in VAFL [4], applying the same DP mechanism to both VFL-CZOFO and ZOO-VFL, which involves clipping the embeddings and adding calibrated vector noise. While VAFL updates server and client once for every communication round, some first-order VFL methods adopt multiple local updates in one communication round [3, 24]. In this paper, we only focus on the same update behavior as VAFL. In addition, model delay has been manually adjusted for all methods based on the per-batch computation time on a single client to simulate client heterogeneity and ensure a fair comparison.

Comparison with Baselines. Figure 2 presents the performance evaluation of DPZV against all baselines on image classification tasks under certain DP levels. The results show that DPZV consistently outperforms all baselines on MNIST and CIFAR-10 under strict privacy budget ($\epsilon = 1$, $\delta = 1 \times 10^{-3}$). On ModelNet40, where training is more challenging due to larger models and a greater number of clients, we slightly relax the DP constraint ($\epsilon = 10$), and observe that DPZV maintains a competitive advantage over other ZO-based methods while achieving accuracy comparable to the first-order baseline VAFL. The scalar noise injected in DPZV effectively constrains the noise magnitude, mitigating the instability typically introduced by noisy zeroth-order gradient estimators. This leads to more stable training dynamics than other ZO based methods. Moreover, in contrast to the high-dimensional vector noise used in first-order baseline VAFL, scalar noise incurs significantly less loss, resulting in superior performance under stringent privacy budgets.

Privacy-Accuracy Tradeoff. Figure 3 presents the accuracy-privacy tradeoff across four benchmark datasets: MNIST, CIFAR-10, ModelNet40, and Amazon Reviews. We evaluate the robustness of our proposed method DPZV under various privacy budgets ϵ , while fixing the failure probability

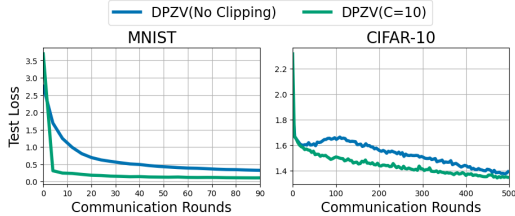


Figure 4: Effect of gradient clipping on DPZV under non-private settings. We compare models trained with and without clipping of the ZO information. Across both MNIST and CIFAR-10, clipping accelerates convergence and stabilizes training.

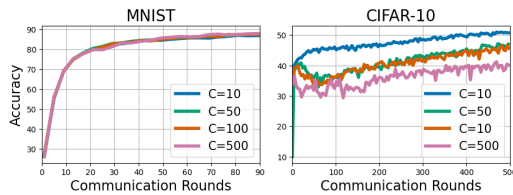


Figure 5: Effect of clipping threshold on DPZV under differential privacy constraint $\epsilon = 1$. While all clipping levels perform similarly on MNIST, smaller thresholds ($C = 10$) significantly improve accuracy and convergence on CIFAR-10.

$\delta = 1 \times 10^{-3}$. Across all tasks, DPZV consistently achieves the highest accuracy under tight privacy regimes ($\epsilon \leq 1$), indicating its ability to maintain model utility even with stringent differential privacy constraints. Notably, on MNIST and ModelNet40, DPZV shows only a marginal drop in accuracy as ϵ decreases, while the competing methods suffer substantial degradation. For instance, on CIFAR-10 at $\epsilon = 0.1$, DPZV maintains over 90% accuracy, whereas ZOF0 and ZOO-VFL fall below 30%. Similar trends are observed on Amazon Reviews, where DPZV consistently outperforms baselines under strict privacy, especially at $\epsilon = 1$ and $\epsilon = 5$. These results validate the effectiveness of our scalar-noise-based DP mechanism in balancing utility and privacy, and *highlight its advantage in real-world privacy-sensitive federated learning scenarios*.

Effect of Clipping in Non-Private Scenarios. We observe in Figure 3 that even under no privacy constraints ($\epsilon = \infty$), DPZV outperforms other ZO based algorithms. A key distinction lies in DPZV’s use of scalar clipping on ZO information, while originally introduced for differential privacy, also acts as a form of gradient regularization. This regularization effect has been shown to improve convergence in prior work [37], and we observe similar benefits here. Figure 4 verifies our insight by comparing the convergence behavior of DPZV with and without gradient clipping under a non-private setting. The plots show test loss versus communication rounds. In both datasets, applying clipping to the ZO information significantly improves convergence speed. For MNIST, clipped DPZV reaches low test loss much faster and stabilizes more smoothly. On CIFAR-10, the clipped version also demonstrates consistently lower loss throughout training. These results suggest that clipping not only stabilizes training but also enhances convergence efficiency, even when privacy is not enforced.

Impact of Sensitivity Level. Figure 5 presents the performance of DPZV under different sensitivity levels, which is controlled by the clipping threshold C . We apply a fixed privacy budget of $\epsilon = 1$, $\delta = 1 \times 10^{-3}$ on both MNIST and CIFAR-10. In the MNIST setting, all clipping levels achieve similar convergence and final accuracy, suggesting the model is robust to the choice of C in simple tasks. In contrast, the CIFAR-10 results highlight a pronounced impact: smaller clipping values (e.g., $C = 10$) yield better accuracy and stability over training. Larger thresholds, such as $C = 500$ degrade performance, likely due to the excessive noise required to satisfy DP constraints. These results emphasize the importance of careful clipping calibration in more complex settings to ensure a good privacy-utility tradeoff.

8 Conclusion and Limitations

In this work, we propose DPZV, the first zero-order VFL framework that achieves robust and controllable privacy guarantees while maintaining strong model utility. Through rigorous theoretical analysis, we establish the strong convergence properties of our algorithm. Extensive experiments demonstrate that DPZV outperforms all baselines across various privacy levels and cost evaluations. Our method also features a lightweight memory footprint, enabling enhanced performance on large language models. These results provide valuable insights for future advancements in VFL and distributed ZO optimization methods.

We identify several potential limitations of our work. Notably, the convergence rate established in our theoretical analysis remains dimension-dependent, consistent with prior results in centralized ZO optimization. Extending the dimension-free convergence guarantees shown in [26] to the VFL setting poses a nontrivial challenge due to the inherently distributed and feature-partitioned nature of VFL. Investigating such extensions is a promising direction for future work.

References

- [1] Martin Abadi, Andy Chu, Ian Goodfellow, H Brendan McMahan, Ilya Mironov, Kunal Talwar, and Li Zhang. Deep learning with differential privacy. In *Proceedings of the 2016 ACM SIGSAC conference on computer and communications security*, pages 308–318, 2016.
- [2] Giuseppe Ateniese, Luigi V Mancini, Angelo Spognardi, Antonio Villani, Domenico Vitali, and Giovanni Felici. Hacking smart machines with smarter ones: How to extract meaningful data from machine learning classifiers. *International Journal of Security and Networks*, 10(3):137–150, 2015.
- [3] Timothy Castiglia, Shiqiang Wang, and Stacy Patterson. Flexible vertical federated learning with heterogeneous parties. *IEEE Transactions on Neural Networks and Learning Systems*, 2023.
- [4] Tianyi Chen, Xiao Jin, Yuejiao Sun, and Wotao Yin. Vaf: a method of vertical asynchronous federated learning. *arXiv preprint arXiv:2007.06081*, 2020.
- [5] Xiangyi Chen, Steven Z Wu, and Mingyi Hong. Understanding gradient clipping in private sgd: A geometric perspective. *Advances in Neural Information Processing Systems*, 33:13773–13782, 2020.
- [6] Kewei Cheng, Tao Fan, Yilun Jin, Yang Liu, Tianjian Chen, Dimitrios Papadopoulos, and Qiang Yang. Secureboost: A lossless federated learning framework. *IEEE intelligent systems*, 36(6):87–98, 2021.
- [7] Li Deng. The mnist database of handwritten digit images for machine learning research [best of the web]. *IEEE signal processing magazine*, 29(6):141–142, 2012.
- [8] Jacob Devlin. Bert: Pre-training of deep bidirectional transformers for language understanding. *arXiv preprint arXiv:1810.04805*, 2018.
- [9] Jinshuo Dong, Aaron Roth, and Weijie J Su. Gaussian differential privacy. *Journal of the Royal Statistical Society: Series B (Statistical Methodology)*, 84(1):3–37, 2022.
- [10] Cynthia Dwork, Frank McSherry, Kobbi Nissim, and Adam Smith. Calibrating noise to sensitivity in private data analysis. In *Theory of Cryptography: Third Theory of Cryptography Conference, TCC 2006, New York, NY, USA, March 4-7, 2006. Proceedings 3*, pages 265–284. Springer, 2006.
- [11] Cynthia Dwork, Aaron Roth, et al. The algorithmic foundations of differential privacy. *Foundations and Trends® in Theoretical Computer Science*, 9(3–4):211–407, 2014.
- [12] Wenzhi Fang, Ziyi Yu, Yuning Jiang, Yuanming Shi, Colin N Jones, and Yong Zhou. Communication-efficient stochastic zeroth-order optimization for federated learning. *IEEE Transactions on Signal Processing*, 70:5058–5073, 2022.
- [13] Chong Fu, Xuhong Zhang, Shouling Ji, Jinyin Chen, Jingzheng Wu, Shanqing Guo, Jun Zhou, Alex X Liu, and Ting Wang. Label inference attacks against vertical federated learning. In *31st USENIX security symposium (USENIX Security 22)*, pages 1397–1414, 2022.
- [14] Saeed Ghadimi and Guanghui Lan. Stochastic first-and zeroth-order methods for nonconvex stochastic programming. *SIAM journal on optimization*, 23(4):2341–2368, 2013.
- [15] Stephen Hardy, Wilko Henecka, Hamish Ivey-Law, Richard Nock, Giorgio Patrini, Guillaume Smith, and Brian Thorne. Private federated learning on vertically partitioned data via entity resolution and additively homomorphic encryption. *arXiv preprint arXiv:1711.10677*, 2017.
- [16] Zecheng He, Tianwei Zhang, and Ruby B Lee. Model inversion attacks against collaborative inference. In *Proceedings of the 35th Annual Computer Security Applications Conference*, pages 148–162, 2019.
- [17] Yaochen Hu, Di Niu, Jianming Yang, and Shengping Zhou. Fdml: A collaborative machine learning framework for distributed features. In *Proceedings of the 25th ACM SIGKDD International Conference on Knowledge Discovery & Data Mining*, pages 2232–2240, 2019.
- [18] Xue Jiang, Xuebing Zhou, and Jens Grossklags. Comprehensive analysis of privacy leakage in vertical federated learning during prediction. *Proceedings on Privacy Enhancing Technologies*, 2022.
- [19] Xiao Jin, Pin-Yu Chen, Chia-Yi Hsu, Chia-Mu Yu, and Tianyi Chen. Cafe: Catastrophic data leakage in vertical federated learning. *Advances in Neural Information Processing Systems*, 34:994–1006, 2021.
- [20] Alex Krizhevsky, Geoffrey Hinton, et al. Learning multiple layers of features from tiny images. 2009.
- [21] Oscar Li, Jiankai Sun, Xin Yang, Weihao Gao, Hongyi Zhang, Junyuan Xie, Virginia Smith, and Chong Wang. Label leakage and protection in two-party split learning. *arXiv preprint arXiv:2102.08504*, 2021.
- [22] Jiandong Liu, Lan Zhang, Xiaojing Yu, and Xiang-Yang Li. Differentially private distributed online convex optimization towards low regret and communication cost. In *Proceedings of the Twenty-fourth International Symposium on Theory, Algorithmic Foundations, and Protocol Design for Mobile Networks and Mobile Computing*, pages 171–180, 2023.
- [23] Yang Liu, Yan Kang, Tianyuan Zou, Yanhong Pu, Yuanqin He, Xiaozhou Ye, Ye Ouyang, Ya-Qin Zhang, and Qiang Yang. Vertical federated learning: Concepts, advances, and challenges. *IEEE Transactions on Knowledge and Data Engineering*, 2024.

- [24] Yang Liu, Xinwei Zhang, Yan Kang, Liping Li, Tianjian Chen, Mingyi Hong, and Qiang Yang. Fedbcd: A communication-efficient collaborative learning framework for distributed features. *IEEE Transactions on Signal Processing*, 70:4277–4290, 2022.
- [25] Xinjian Luo, Yuncheng Wu, Xiaokui Xiao, and Beng Chin Ooi. Feature inference attack on model predictions in vertical federated learning. In *2021 IEEE 37th International Conference on Data Engineering (ICDE)*, pages 181–192. IEEE, 2021.
- [26] Sadhika Malladi, Tianyu Gao, Eshaan Nichani, Alex Damian, Jason D Lee, Danqi Chen, and Sanjeev Arora. Fine-tuning language models with just forward passes. *Advances in Neural Information Processing Systems*, 36:53038–53075, 2023.
- [27] Julian McAuley and Jure Leskovec. Hidden factors and hidden topics: understanding rating dimensions with review text. In *Proceedings of the 7th ACM conference on Recommender systems*, pages 165–172, 2013.
- [28] Yurii Nesterov and Vladimir Spokoiny. Random gradient-free minimization of convex functions. *Foundations of Computational Mathematics*, 17(2):527–566, 2017.
- [29] Nicolas Papernot, Patrick McDaniel, Arunesh Sinha, and Michael P Wellman. Sok: Security and privacy in machine learning. In *2018 IEEE European symposium on security and privacy (EuroS&P)*, pages 399–414. IEEE, 2018.
- [30] Ohad Shamir. An optimal algorithm for bandit and zero-order convex optimization with two-point feedback. *Journal of Machine Learning Research*, 18(52):1–11, 2017.
- [31] Xicong Shen, Ying Liu, and Zhaoyang Zhang. Performance-enhanced federated learning with differential privacy for internet of things. *IEEE Internet Things J.*, 9(23):24079–24094, 2022.
- [32] Xinyu Tang, Ashwinee Panda, Milad Nasr, Saeed Mahloujifar, and Prateek Mittal. Private fine-tuning of large language models with zeroth-order optimization. *arXiv preprint arXiv:2401.04343*, 2024.
- [33] Ganyu Wang, Bin Gu, Qingsong Zhang, Xiang Li, Boyu Wang, and Charles X Ling. A unified solution for privacy and communication efficiency in vertical federated learning. *Advances in Neural Information Processing Systems*, 36, 2024.
- [34] Zhirong Wu, Shuran Song, Aditya Khosla, Fisher Yu, Linguang Zhang, Xiaoou Tang, and Jianxiong Xiao. 3d shapenets: A deep representation for volumetric shapes. In *Proceedings of the IEEE conference on computer vision and pattern recognition*, pages 1912–1920, 2015.
- [35] Chulin Xie, Pin-Yu Chen, Qinbin Li, Arash Nourian, Ce Zhang, and Bo Li. Improving privacy-preserving vertical federated learning by efficient communication with admm. In *2024 IEEE Conference on Secure and Trustworthy Machine Learning (SaTML)*, pages 443–471. IEEE, 2024.
- [36] Peng Ye, Zhifeng Jiang, Wei Wang, Bo Li, and Baochun Li. Feature reconstruction attacks and countermeasures of dnn training in vertical federated learning. *IEEE Transactions on Dependable and Secure Computing*, 2024.
- [37] Jingzhao Zhang, Tianxing He, Suvrit Sra, and Ali Jadbabaie. Why gradient clipping accelerates training: A theoretical justification for adaptivity. *arXiv preprint arXiv:1905.11881*, 2019.
- [38] Liang Zhang, Bingcong Li, Kiran Koshy Thekumparampil, Sewoong Oh, and Niao He. Dpzero: Private fine-tuning of language models without backpropagation. In *Forty-first International Conference on Machine Learning*, 2024.
- [39] Qingsong Zhang, Bin Gu, Zhiyuan Dang, Cheng Deng, and Heng Huang. Desirable companion for vertical federated learning: New zeroth-order gradient based algorithm. In *Proceedings of the 30th ACM International Conference on Information & Knowledge Management*, pages 2598–2607, 2021.
- [40] Yang Zhao, Jun Zhao, Mengmeng Yang, Teng Wang, Ning Wang, Lingjuan Lyu, Dusit Niyato, and Kwok-Yan Lam. Local differential privacy-based federated learning for internet of things. *IEEE Internet Things J.*, 8(11):8836–8853, 2021.
- [41] Tianyuan Zou, Yang Liu, Yan Kang, Wenhan Liu, Yuanqin He, Zhihao Yi, Qiang Yang, and Ya-Qin Zhang. Defending batch-level label inference and replacement attacks in vertical federated learning. *IEEE Transactions on Big Data*, 2022.

Appendix

A Preliminaries and Outline	13
B Proof of Convergence Theorem 5.4	16
C Proof of Differential Privacy Theorem 6.1	18
D Intermediate Lemmas	19
E Discussion of Differential Privacy under Various Settings	24
E.1 Protection Against an Honest-but-Curious Threat Model	25
E.2 Protection Against Post-Training Attacks	25
F Memory Cost	25
G Choice of all Hyperparameters	26

A Preliminaries and Outline

We first define the following notation table to facilitate the proof:

Notation	Description
$\mathbf{w} = [w_0, w_1, w_2, \dots, w_M]$	All learnable parameters
d_0, d_1, \dots, d_M	Dimension of parameters on server (machine 0) and client $1, \dots, M$
$d = \sum_{m=0}^M d_m$	Dimension of all parameters
$f(\mathbf{w}; \xi_i) := \mathcal{L}(w_0, h_{1,i}, h_{2,i}, \dots, h_{M,i}; y_i)$	Loss function with regard to datum with ID i
$F(\mathbf{w}) := F(\mathbf{w}; \mathcal{D}, \mathbf{Y})$	Global loss function
$\chi^t = [w_1^{t_1}, \dots, w_M^{t_M}]$	Latest learnable parameters of all clients at server time t
$\tilde{\chi}^t = [w_1^{t_1 - \tau_1^t}, \dots, w_M^{t_M - \tau_M^t}]$	Delayed learnable parameters of all clients at server time t
$\mathbf{w}^t = [w_0^t, w_1^{t_1}, \dots, w_M^{t_M}]$	Latest learnable parameters of all clients and the server at server time t
$\tilde{\mathbf{w}}^t = [w_0^{t - \tau_1^t}, w_1^{t_1 - \tau_1^t}, \dots, w_M^{t_M - \tau_M^t}]$	Delayed learnable parameters of all clients and the server at server time t
$h_{m,i}^{\pm} = h_m(w_m^{t_m} \pm \lambda_m \mathbf{u}_m^{t_m}; \xi_{m,i})$	Local embeddings of client m for data sample i at client time t_m under the perturbed parameters
$\delta_{m,i}^{t,t_m}$ as defined in (7)	zeroth-order difference information from client m and data sample i at server time t and client time t_m
$g_{m,i}^t(\tilde{\mathbf{w}}^t) = \delta_{m,i}^{t,t_m} \mathbf{u}_m^{t_m}$	zeroth-order gradient estimator from client m and data sample i at server time t (with delay)
$\check{g}_{m,i}^t(\tilde{\mathbf{w}}^t) = \text{clip}_C(\delta_{m,i}^{t,t_m}) \mathbf{u}_m^{t_m}$	Clipped zeroth-order gradient estimator from client m and data sample i at server time t (with delay)
$\check{G}_m^t(\tilde{\mathbf{w}}^t) = (1/B) \sum_{i \in \mathcal{I}_m^{t_m}} \check{g}_{m,i}^t(\tilde{\mathbf{w}}^t) + z_m^{t_m} \mathbf{u}_m^{t_m}$	Clipped differential private zeroth-order gradient estimator from client m at server time t (with delay)
$G_m^t(\tilde{\mathbf{w}}^t) = (1/B) \sum_{i \in \mathcal{I}_m^{t_m}} g_{m,i}^t(\tilde{\mathbf{w}}^t) + z_m^{t_m} \mathbf{u}_m^{t_m}$	Non-clipped differential private zeroth-order gradient estimator from client m at server time t (with delay)

Table 1: Table of Notations

Note that in the notation table, we use “ $\check{\cdot}$ ” to define clipped gradient estimators, and we use “ $\tilde{\cdot}$ ” to denote delayed model parameters. In the rest of the proof, we also use gradient estimators parameterized by the no delaying parameters \mathbf{w} instead of $\tilde{\mathbf{w}}$ to assume that we update the model without delay.

To begin with, we restate the assumptions required for establishing the convergence analysis.

Assumption A.1 (ℓ -Lipschitz). The function $f(\mathbf{w}; \xi)$ is ℓ -Lipschitz continuous for every ξ .

Assumption A.2 (L -Smooth). The function $f(\mathbf{w}; \xi)$ is L -Smooth for every ξ . Specifically, there exists an $L > 0$ for all $m = 0, \dots, M$ such that $\|\nabla_{w_m} f(\mathbf{w}) - \nabla_{w_m} f(\mathbf{w}')\| \leq L \|\mathbf{w} - \mathbf{w}'\|$.

Assumption A.3 (Bounded gradient variance). The variance of the stochastic first order gradient is upper bounded in expectation:

$$\mathbb{E} \left[\|\nabla_{\mathbf{w}} f(\mathbf{w}; \xi) - \nabla_{\mathbf{w}} F(\mathbf{w})\|^2 \right] \leq \sigma_s^2$$

Assumption A.4 (Independent Participation). The probability of one client participating in one communication round is independent of other clients and satisfies

$$\mathbb{P}(\text{client } m \text{ uploading}) = q_m$$

Specially, we set $q_0 = 1$ as the server always participates in the update.

One of the important parts in the proof of Theorem 5.4 is to bound the zeroth-order gradient estimator. We first introduce the formal definition of zeroth-order two-point gradient estimator that is used in our algorithm, and prove some technical lemmas that reveal some important properties.

Definition A.5. Let \mathbf{u} be uniformly sampled from the Euclidean sphere $\sqrt{d}\mathbb{S}^{d-1}$. For any function $f(x) : \mathbb{R}^d \rightarrow \mathbb{R}$ and $\lambda > 0$, we define its zeroth-order gradient estimator as

$$g(\mathbf{w}) = \frac{(f(\mathbf{w} + \lambda\mathbf{u}) - f(\mathbf{w} - \lambda\mathbf{u}))}{2\lambda}\mathbf{u} \quad (12)$$

Lemma A.6. Let $g(\mathbf{w})$ be the zeroth-order gradient estimator defined as in (12), with $f(\mathbf{w})$ being the loss function. We define the smoothed function $f_\lambda(\mathbf{w}) = \mathbb{E}_{\mathbf{u}}[f(\mathbf{w} + \lambda\mathbf{u})]$, where v is uniformly sampled from the Euclidean ball $\sqrt{d}\mathbb{B}^d = \{\mathbf{w} \in \mathbb{R}^d \mid \|\mathbf{w}\| \leq \sqrt{d}\}$. The following properties hold:

(i) $f_\lambda(\mathbf{w})$ is differentiable and $\mathbb{E}_{\mathbf{u}}[g(\mathbf{w})] = \nabla f_\lambda(\mathbf{w})$.

(ii) If $f(\mathbf{w})$ is L -smooth, we have that

$$\|\nabla f(\mathbf{w}) - \nabla f_\lambda(\mathbf{w})\| \leq \frac{L}{2}\lambda d^{3/2}, \quad (13)$$

$$|f(\mathbf{w}) - f_\lambda(\mathbf{w})| \leq \frac{L}{2}\lambda^2 d, \quad (14)$$

and

$$\mathbb{E}_{\mathbf{u}}[\|g_\lambda(\mathbf{w})\|^2] \leq 2d \cdot \|\nabla f(\mathbf{w})\|^2 + \frac{L^2}{2}\lambda^2 d^3. \quad (15)$$

Based on (14), we can further show:

$$\|\nabla f_\lambda(\mathbf{w})\|^2 \leq 2\|\nabla f(\mathbf{w})\|^2 + \frac{L^2}{2}\lambda^2 d^3 \quad (16)$$

$$\|\nabla f(\mathbf{w})\|^2 \leq 2\|\nabla f_\lambda(\mathbf{w})\|^2 + \frac{L^2}{2}\lambda^2 d^3 \quad (17)$$

This is the standard result of zeroth-order optimization. The proof of the Lemma is given by [28]

We also find the following lemmas useful in the proof:

Lemma A.7. Let \mathbf{u} be uniformly sampled from the Euclidean sphere $\sqrt{d}\mathbb{S}^{d-1}$, and \mathbf{a} be any vector of constant value. We have that $\mathbb{E}[\mathbf{u}] = 0$ and

$$\mathbb{P}(|\mathbf{u}^\top \mathbf{a}| \geq C) \leq 2\sqrt{2\pi} \exp\left(-\frac{C^2}{8\|\mathbf{a}\|^2}\right).$$

Proof. This lemma follows exactly from Lemma C.1. in [38]. \square

Lemma A.8. Let Q be the event that clipping happened for a sample ξ , d be the model dimension, and L, ℓ be the Lipschitz and smooth constant as defined in Theorem A.1 and Theorem A.2. For $\forall C_0 > 0$, if the clipping threshold C follows $C \geq C_0 + L\lambda d/2$, we have the following upper bound for the probability of clipping:

$$P = \mathbb{P}(Q) \leq 2\sqrt{2\pi} \exp(-\frac{C_0^2}{8\ell^2}) = \Xi \quad (18)$$

Proof. Since $f(\mathbf{u}; \xi)$ is L -Smooth for every ξ , we have

$$\begin{aligned} \left| \frac{f(\mathbf{w} + \lambda\mathbf{u}; \xi) - f(\mathbf{w} - \lambda\mathbf{u}; \xi)}{2\lambda} \right| &\leq |\mathbf{u}^\top \nabla f(\mathbf{w}; \xi)| + \frac{|f(\mathbf{w} + \lambda\mathbf{u}; \xi) - f(\mathbf{w}; \xi) - \lambda\mathbf{u}^\top \nabla f(\mathbf{w}; \xi)|}{2\lambda} \\ &\quad + \frac{|f(\mathbf{w} - \lambda\mathbf{u}; \xi) - f(\mathbf{w}; \xi) + \lambda\mathbf{u}^\top \nabla f(\mathbf{w}; \xi)|}{2\lambda} \end{aligned}$$

$$\leq |\mathbf{u}^\top \nabla f(\mathbf{w}; \xi)| + \frac{L}{2}\lambda.$$

Therefore, by Theorem A.7 and Theorem A.1, we obtain

$$\begin{aligned} \mathbb{P}(Q) &= \mathbb{P}\left(\frac{|f(\mathbf{w} + \lambda\mathbf{u}; \xi_i) - f(\mathbf{w} - \lambda\mathbf{u}; \xi_i)|}{2\lambda} \geq C_0 + \frac{L}{2}\lambda\right) \\ &\leq \mathbb{P}(|\mathbf{u}^\top \nabla f(\mathbf{w}; \xi_i)| \geq C_0) \\ &\leq 2\sqrt{2\pi} \exp\left(-\frac{C_0^2}{8\|\nabla f(\mathbf{w}; \xi_i)\|^2}\right) \\ &\leq 2\sqrt{2\pi} \exp\left(-\frac{C_0^2}{8\ell^2}\right). \end{aligned}$$

□

Lemma A.9 (Expectation and Variance of Clipped Zeroth-order Gradient Estimator). *Recall that $\check{g}_{m,i}^t(\mathbf{w}^t)$ is defined as the clipped zeroth-order gradient estimator assuming no communication delay, random perturbation \mathbf{u} is defined in Theorem A.7, and event Q is defined in Theorem A.8. We have the following properties:*

(i) *When taking expectation w.r.t \mathbf{u} and Q , the clipped zeroth-order gradient estimator follows*

$$\mathbb{E}_{\mathbf{u}}[\check{g}_{m,i}^t(\mathbf{w}^t)] = (1 - P)\nabla_{w_m} F_\lambda(\mathbf{w}^t) \quad (19)$$

(ii) *The variance of $\check{g}_{m,i}^t(\mathbf{w}^t)$ follows*

$$\text{Var}(\check{g}_{m,i}^t(\mathbf{w}^t)) \leq (1 - P)(2d_m\|\nabla_{w_m} F(\mathbf{w}^t)\|^2 + 2d_m\sigma_s^2 + \frac{L^2}{2}\lambda^2 d_m^3) + PC^2 d_m - (1 - P)^2\|\nabla_{w_m} F_\lambda(\mathbf{w}^t)\|^2 \quad (20)$$

Proof. For (i), we have

$$\begin{aligned} \mathbb{E}[\check{g}_{m,i}^t(\mathbf{w}^t)] &= \mathbb{E}[\check{g}_{m,i}^t(\mathbf{w}^t)|\bar{Q}] \mathbb{P}(\bar{Q}) + \mathbb{E}[\check{g}_{m,i}^t(\mathbf{w}^t)|Q] \mathbb{P}(Q) \\ &= \mathbb{E}[\tilde{g}_{m,i}^t(\mathbf{w}^t)] (1 - \mathbb{P}(Q)) + \mathbb{E}[C\mathbf{u}_m^t] \mathbb{P}(Q) \\ &= (1 - P)\nabla_{w_m} F_\lambda(\mathbf{w}^t) \end{aligned}$$

where in the first step we applied the Law of Total Expectation, and in the last step we used the property (i) in Theorem A.6 and (i) in Theorem A.7.

By (19), we can further bound the variance of $\check{g}_{m,i}^t$

$$\begin{aligned} &\text{Var}(\check{g}_{m,i}^t(\mathbf{w}^t)) \\ &= \mathbb{E}\left[\|\check{g}_{m,i}^t(\mathbf{w}^t) - (1 - P)\nabla_{w_m} F_\lambda(\mathbf{w}^t)\|^2\right] \\ &= \mathbb{E}\left[\|\check{g}_{m,i}^t(\mathbf{w}^t)\|^2\right] - (1 - P)^2\|\nabla_{w_m} F_\lambda(\mathbf{w}^t)\|^2 \\ &= \mathbb{E}\left[\|\check{g}_{m,i}^t(\mathbf{w}^t)\|^2|\bar{Q}\right] \mathbb{P}(\bar{Q}) + \mathbb{E}\left[C^2\|\mathbf{u}_m^t\|^2|Q\right] \mathbb{P}(Q) - (1 - P)^2\|\nabla_{w_m} F_\lambda(\mathbf{w}^t)\|^2 \\ &\stackrel{1)}{\leq} (1 - P)(2d_m\|\nabla_{w_m} f(\mathbf{w}^t; \xi_{m,t})\|^2 + \frac{L^2}{2}\lambda^2 d_m^3) \\ &\quad + PC^2 d_m - (1 - P)^2\|\nabla_{w_m} F_\lambda(\mathbf{w}^t)\|^2 \\ &\stackrel{2)}{\leq} (1 - P)(2d_m\|\nabla_{w_m} F(\mathbf{w}^t)\|^2 + 2d_m\sigma_s^2 + \frac{L^2}{2}\lambda^2 d_m^3) \\ &\quad + PC^2 d_m - (1 - P)^2\|\nabla_{w_m} F_\lambda(\mathbf{w}^t)\|^2 \end{aligned}$$

where 1) is by the property of zeroth-order gradient estimator (15) and 2) follows from the bounded gradient assumption (Assumption A.3). □

Lemma A.10 (Bounds on the variance of DP Zeroth-order Gradient Estimator). *Let $\check{G}_m^t(\mathbf{w}^t)$ be the Differential Private Zeroth-order Gradient without delay. Under the same condition as Theorem A.6, we can bound the variance of $\check{G}_m^t(\mathbf{w}^t)$ in expectation, with the expectation taken on random direction \mathbf{u} , DP noise z , and clipping event Q :*

$$\begin{aligned} \text{Var}(\check{G}_m^t(\mathbf{w}^t)) &\leq \frac{1-P}{B} (2d_m \mathbb{E} [\|\nabla_{w_m} F(\mathbf{w}^t)\|^2] + 2d_m \sigma_s^2 + \frac{L^2}{2} \lambda^2 d_m^3) + \frac{P}{B} C^2 d_m \\ &\quad - \frac{(1-P)^2}{B} \mathbb{E} [\|\nabla_{w_m} F_\lambda(\mathbf{w}^t)\|^2] + \sigma_{dp}^2 d_m \end{aligned} \quad (21)$$

Proof. First we show that the expectation on $\check{G}_m^t(\mathbf{w}^t)$ can be written as:

$$\mathbb{E}_u[\check{G}_m^t(\mathbf{w}^t)] = \frac{1}{B} \sum_{i \in \mathcal{I}_m^t} \mathbb{E} [\check{g}_{m,i}^t(\mathbf{w}^t)] + \mathbb{E} [z_m^t \mathbf{u}_m^t] = (1-P) \nabla_{w_m} F_\lambda(\mathbf{w}^t)$$

Thus, the variance can be bounded by:

$$\begin{aligned} &\text{Var}(\check{G}_m^t(\mathbf{w}^t)) \\ &= \mathbb{E} \left[\left\| \check{G}_m^t(\mathbf{w}^t) - (1-P) \nabla_{w_m} F_\lambda(\mathbf{w}^t) \right\|^2 \right] \\ &= \mathbb{E} \left[\left\| \frac{1}{B} \sum_{i \in \mathcal{I}_m^t} (\check{g}_{m,i}^t(\mathbf{w}^t) - (1-P) \nabla_{w_m} F_\lambda(\mathbf{w}^t)) + z_m^t \mathbf{u}_m^t \right\|^2 \right] \\ &= \frac{1}{B^2} \sum_{i \in \mathcal{I}_m^t} \mathbb{E} \left[\left\| \check{g}_{m,i}^t(\mathbf{w}^t) - (1-P) \nabla_{w_m} F_\lambda(\mathbf{w}^t) \right\|^2 \right] + \mathbb{E} \left[\|z_m^t \mathbf{u}_m^t\|^2 \right] \\ &\stackrel{(a)}{\leq} \frac{1-P}{B} (2d_m \mathbb{E} [\|\nabla_{w_m} F(\mathbf{w}^t)\|^2] + 2d_m \sigma_s^2 + \frac{L^2}{2} \lambda^2 d_m^3) + \frac{P}{B} C^2 d_m - \frac{(1-P)^2}{B} \mathbb{E} [\|\nabla_{w_m} F_\lambda(\mathbf{w}^t)\|^2] + \sigma_{dp}^2 d_m, \end{aligned}$$

where (a) follows from (20). \square

Finally, for analyzing the delayed information in model parameter, we define the following Lyapunov function:

$$V^t = F(\mathbf{w}^t) + \sum_{i=1}^{\tau} \gamma_i \|\chi^{t+1-i} - \chi^{t-i}\|^2 \quad (22)$$

with γ_i to be determined later.

B Proof of Convergence Theorem 5.4

We first state the full version of the main convergence Theorem 5.4.

Theorem B.1. *Under Theorem A.1 to A.4, and assume the client delay τ_m is uniformly upper bounded by τ . If we denote $q_* = \min_m q_m$, $d_* = \max_m d_m$, and let $\eta_0 = \eta_m = \eta \leq \min\{\frac{1}{\sqrt{T d_*}}, \frac{B}{4L(B+8d_0)+8\gamma_1(2d_m+B)}\}$, $\lambda \leq \frac{1}{Ld\sqrt{T}}$, we have the following theorem:*

$$\begin{aligned} \frac{1}{T} \sum_{t=0}^{T-1} \mathbb{E} [\|\nabla_{\mathbf{w}} F(\mathbf{w}^t)\|^2] &\leq \frac{1}{1-\Xi} \left\{ \frac{8\sqrt{d_*}}{q_* T^{1/2}} \mathbb{E} [F^0 - F^T] + \frac{2d_*}{q_* T} + \frac{8\sqrt{d_*}}{q_* L d T^{1/2}} + \frac{16(4L+2\gamma_1)\sqrt{d_*} \sigma_s^2}{q_* B T^{1/2}} \right. \\ &\quad \left. + \frac{4((4-B)L + (B+2)\gamma_1)\sqrt{d_*}}{q_* B T^{1/2}} + \frac{16(2L+\gamma_1)\Xi C^2 \sqrt{d_*}}{q_* B T^{1/2}} + \frac{16(2L+\gamma_1)\sigma_{dp}^2 d_m}{q_* T^{1/2} \sqrt{d_*}} \right\}, \end{aligned} \quad (23)$$

where $\Xi = 2\sqrt{2\pi} \exp(-\frac{C^2}{8\ell^2})$.

Proof. We start from the result of an intermediate Theorem D.2, which quantifies the descent of the Lyapunov function, and we relegate the proof to Appendix D.

$$\mathbb{E} [V^{t+1} - V^t] \leq -\frac{1-P}{8} \min_m \{q_m \eta_m\} \mathbb{E} \left[\|\nabla_{\mathbf{w}} F(\mathbf{w}^t)\|^2 \right] + \mathcal{A}_1 + \mathcal{A}_2 \quad (24)$$

Note that \mathcal{A}_1 and \mathcal{A}_2 are constant terms defined in (35) and (39).

We first re-arranging the terms in (24), and take average over $0, 1, \dots, T-1$:

$$\begin{aligned} & \frac{1-P}{8T} \min_m \{q_m \eta_m\} \sum_{t=0}^{T-1} \mathbb{E} \left[\|\nabla_{\mathbf{w}} F(\mathbf{w}^t)\|^2 \right] \\ & \leq \frac{1}{T} \mathbb{E} [V^0 - V^T] + \mathcal{A}_1 + \mathcal{A}_2 \\ & \leq \frac{1}{T} \mathbb{E} [F^0 - F^T] + \mathcal{A}_1 + \mathcal{A}_2, \end{aligned}$$

where the second inequality follows from the definition of V^t in (22).

Dividing $\alpha = \frac{1}{8} \min_m \{q_m \eta_m\}$ from both sides, and plugging in \mathcal{A}_1 and \mathcal{A}_2 , we have:

$$\begin{aligned} & \frac{1-P}{T} \sum_{t=0}^{T-1} \mathbb{E} \left[\|\nabla_{\mathbf{w}} F(\mathbf{w}^t)\|^2 \right] \\ & \leq \frac{1}{\alpha T} \mathbb{E} [F^0 - F^T] + \frac{1}{\alpha} \sum_{m=0}^M q_m \eta_m \frac{L^2}{8} \lambda^2 d_m^3 \\ & \quad + \frac{1}{\alpha} \sum_{m=0}^M q_m \eta_m^2 L \left(\frac{4}{B} d_m \sigma_s^2 + \frac{(4-B)L^2}{4B} \lambda^2 d_m^3 + \frac{2P}{B} C^2 d_m + 2\sigma_{dp}^2 d_m \right) \\ & \quad + \frac{1}{\alpha} L \lambda^2 d + \frac{1}{\alpha} \sum_{m=1}^M q_m \eta_m^2 \gamma_1 \left(\frac{L^2}{4} \lambda^2 d_m^3 + \frac{2}{B} d_m \sigma_s^2 + \frac{L^2}{2B} \lambda^2 d_m^3 + \frac{P}{B} C^2 d_m + \sigma_{dp}^2 d_m \right) \end{aligned}$$

For the simplicity of analysis, we let $\eta_0 = \eta_m = \eta$, $q_* = \min_m q_m$, then $\alpha = \frac{\eta}{8} q_*$. Let $d_* = \max_m d_c$, and $\lambda \leq \frac{1}{Ld\sqrt{T}}$. Thus,

$$\begin{aligned} & \frac{1-P}{T} \sum_{t=0}^{T-1} \mathbb{E} \left[\|\nabla_{\mathbf{w}} F(\mathbf{w}^t)\|^2 \right] \\ & \leq \frac{8}{q_* \eta T} \mathbb{E} [F^0 - F^T] + \frac{2d_*^3/d^2}{q_* T} + \frac{16\eta L}{q_*} \left(\frac{4}{B} d_* \sigma_s^2 + \frac{(4-B)d_*^3/d^2}{4BT} + \frac{2P}{B} C^2 d_* + 2\sigma_{dp}^2 d_* \right) \\ & \quad + \frac{8}{q_* L d \eta T} + \frac{16\eta \gamma_1}{q_*} \left(\frac{2}{B} d_* \sigma_s^2 + \frac{(B+2)d_*^3/d^2}{4BT} + \frac{P}{B} C^2 d_* + \sigma_{dp}^2 d_m \right) \\ & \leq \frac{8}{q_* \eta T} \mathbb{E} [F^0 - F^T] + \frac{2d_*}{q_* T} + \frac{8}{q_* L d \eta T} + \frac{16\eta(4L+2\gamma_1)d_* \sigma_s^2}{q_* B} + \frac{4\eta((4-B)L+(B+2)\gamma_1)d_*}{q_* B T} \\ & \quad + \frac{16\eta(2L+\gamma_1)PC^2 d_*}{q_* B} + \frac{16\eta(2L+\gamma_1)\sigma_{dp}^2 d_*}{q_*} \end{aligned}$$

where in the last step, we use the fact that $d > d_*$.

If we choose $\eta = \frac{1}{\sqrt{Td_*}}$, we can get the convergence rate:

$$\begin{aligned} & \frac{1}{T} \sum_{t=0}^{T-1} \mathbb{E} \left[\|\nabla_{\mathbf{w}} F(\mathbf{w}^t)\|^2 \right] \\ & \leq \frac{1}{1-P} \left\{ \frac{8\sqrt{d_*}}{q_* T^{1/2}} \mathbb{E} [F^0 - F^T] + \frac{2d_*}{q_* T} + \frac{8\sqrt{d_*}}{q_* L d T^{1/2}} + \frac{16(4L+2\gamma_1)\sqrt{d_*} \sigma_s^2}{q_* B T^{1/2}} \right. \\ & \quad \left. + \frac{4((4-B)L+(B+2)\gamma_1)\sqrt{d_*}}{q_* B T^{1/2}} + \frac{16(2L+\gamma_1)PC^2 \sqrt{d_*}}{q_* B T^{1/2}} + \frac{16(2L+\gamma_1)\sigma_{dp}^2 \sqrt{d_*}}{q_* T^{1/2}} \right\} \end{aligned}$$

$$\leq \frac{1}{1 - \Xi} \left\{ \frac{8\sqrt{d_*}}{q_* T^{1/2}} \mathbb{E} [F^0 - F^T] + \frac{2d_*}{q_* T} + \frac{8\sqrt{d_*}}{q_* L d T^{1/2}} + \frac{16(4L + 2\gamma_1)\sqrt{d_*}\sigma_s^2}{q_* B T^{1/2}} \right. \\ \left. + \frac{4((4 - B)L + (B + 2)\gamma_1)\sqrt{d_*}}{q_* B T^{1/2}} + \frac{16(2L + \gamma_1)\Xi C^2 \sqrt{d_*}}{q_* B T^{1/2}} + \frac{16(2L + \gamma_1)\sigma_{dp}^2 \sqrt{d_*}}{q_* T^{1/2}} \right\}$$

where the last step follows by Theorem A.8.

We thus conclude that the convergence rate is

$$\mathcal{O}\left(\frac{d_*^{1/2} \mathbb{E} [F^0 - F^T] + d_*^{1/2} \sigma_s^2 + d_*^{1/2} \sigma_{dp}^2}{T^{1/2}}\right),$$

where constants before terms have been omitted for simplicity. We note that our convergence rate is of the same order compared to centralized ZO optimization under the same smoothness assumption, up to an error term σ_{dp} introduced by Differential Privacy. \square

C Proof of Differential Privacy Theorem 6.1

In this section, we give rigorous proof for the differential privacy guarantee in Theorem 6.1.

We first introduce the definition of Gaussian differential privacy (GDP) [9] which will be useful in the proof for Theorem 6.1. Compared with traditional DP defined in (4), this notion of privacy provides a much tighter composition theorem.

Definition C.1 (Gaussian Differential Privacy). Let $G_\mu := T(\mathcal{N}(0, 1), \mathcal{N}(\mu, 1))$ for $\mu \geq 0$, where the trade-off function $T(P, Q) : [0, 1] \rightarrow [0, 1]$ is defined as $T(P, Q)(\alpha) = \inf(\beta_\phi : \alpha_\phi < \alpha)$. A mechanism M is said to satisfy μ -Gaussian Differential Privacy if it satisfies

$$T(M(X), M(X')) \geq G_\mu$$

For all neighboring dataset $X, X' \in \mathcal{X}^n$.

We construct our DP algorithm based on the Gaussian Mechanism. The Gaussian Mechanism of GDP is given by the following theorem.

Theorem C.2 (Gaussian Mechanism for Gaussian Differential Privacy). *Define the Gaussian mechanism that operates on a statistic θ as $M(\theta) = \theta(X) + \sigma$, where $\sigma \sim \mathcal{N}(0, r^2 C_\theta^2 / \mu^2)$, r is the sample rate for a single datum, and C_θ is the L_2 sensitivity of X . Then, M is μ -GDP.*

The iterative nature of gradient-like algorithms calls for the composition theorem.

Theorem C.3 (Composition of Gaussian Differential Privacy). *The T -fold composition of μ -GDP mechanisms is $\sqrt{T}\mu$ -GDP*

For the ease of comparison, we convert GDP to the common (ϵ, δ) -DP based on the following lossless conversion:

Theorem C.4 (Conversion from Gaussian Differential Privacy to (ϵ, δ) -Differential Privacy). *A mechanism is μ -GDP iff it is $(\epsilon, \delta(\epsilon))$ -DP for all $\epsilon \geq 0$, where*

$$\delta(\epsilon) = \Phi\left(-\frac{\epsilon}{\mu} + \frac{\mu}{2}\right) - e^\epsilon \Phi\left(-\frac{\epsilon}{\mu} - \frac{\mu}{2}\right)$$

The proof of Theorem C.2-C.4 is given in [9].

We are now ready to present the proof for Theorem 6.1.

Proof of Theorem 6.1

Proof. First recall the definition of Δ_m^t defined in (8):

$$\Delta_m^t = \frac{1}{B} \sum_{i \in \mathcal{I}_m^t} \text{clip}_C(\delta_{m,i}^{t,t_m}) + z_m^t$$

For a pair of neighboring dataset X, X' differing in only one entry of data, the L_2 sensitivity C_L of $\frac{1}{B} \sum_{i \in \mathcal{I}_m^t} \text{clip}_C(\delta_{m,i}^{t,t_m})$ follows by

$$C_L = \left\| \frac{1}{B} \sum_{i \in \mathcal{I}_m^t} \text{clip}_C(\delta_{m,i}^{t,t_m}) \right\|_2 \leq \frac{1}{B} \left\| \text{clip}_C(\delta_{m,i}^{t,t_m}) \right\|_2 \leq \frac{2C}{B}$$

The sample rate r of a single data is seen to be the batch size B divided by the size of the dataset D :

$$r = \frac{B}{D}$$

Note that in Theorem 6.1, the standard variance of z_m^t is given by

$$\sigma_{dp} = \frac{2C\sqrt{T}}{D\mu} = \frac{(B/D)(2C/B)\sqrt{T}}{\mu} = \frac{rC_L}{(\mu/\sqrt{T})}$$

By Theorem C.2, the mechanism conducted in (8) satisfies (μ/\sqrt{T}) -Gaussian Differential Privacy. Further applying the composition of GDP in Theorem C.3, and by the post-processing [11] of differential privacy, we have that the whole training process of Algorithm 1 is μ -GDP. We complete the proof by converting μ -GDP to (ϵ, δ) -DP according to Theorem C.4. \square

D Intermediate Lemmas

Lemma D.1 (Model Update With Delay). *Under Theorem A.1 to A.4, we have the following lemma:*

$$\begin{aligned} \mathbb{E} [F(\mathbf{w}^{t+1}) - F(\mathbf{w}^t)] &\leq - \sum_{m=0}^M q_m \eta_m (1-P) \left(\frac{1}{4} - \frac{\eta_m L(B + 8d_m)}{2B} \right) \mathbb{E} \left[\|\nabla_{w_m} F(\mathbf{w}^t)\|^2 \right] \\ &\quad + \sum_{m=0}^M q_m \eta_m L \left(\frac{1}{2} + 2\eta_m L^2 \right) \mathbb{E} \left[\|\tilde{\chi}^t - \chi^t\|^2 \right] + \mathcal{A}_1 \end{aligned} \quad (25)$$

Proof. By Theorem A.2:

$$\begin{aligned} F_\lambda(\mathbf{w}^{t+1}) &\leq F_\lambda(\mathbf{w}^t) + \langle \nabla_{\mathbf{w}} F_\lambda(\mathbf{w}^t), \mathbf{w}^{t+1} - \mathbf{w}^t \rangle + \frac{L}{2} \|\mathbf{w}^{t+1} - \mathbf{w}^t\|^2 \\ &= F_\lambda(\mathbf{w}^t) - \eta_0 \langle \nabla_{w_0} F_\lambda(\mathbf{w}^t), \check{G}_0^t(\tilde{\mathbf{w}}^t) \rangle + \frac{L\eta_0^2}{2} \left\| \check{G}_0^t(\tilde{\mathbf{w}}^t) \right\|^2 \\ &\quad - \eta_m \langle \nabla_{w_m} F_\lambda(\mathbf{w}^t), \check{G}_m^t(\tilde{\mathbf{w}}^t) \rangle + \frac{L\eta_m^2}{2} \left\| \check{G}_m^t(\tilde{\mathbf{w}}^t) \right\|^2 \\ \mathbb{E} [F_\lambda(\mathbf{w}^{t+1})] &\leq \mathbb{E} [F_\lambda(\mathbf{w}^t)] - \underbrace{\eta_0 \mathbb{E} \langle \nabla_{w_0} F_\lambda(\mathbf{w}^t), \check{G}_0^t(\tilde{\mathbf{w}}^t) \rangle}_{\mathcal{E}_1} + \underbrace{\frac{L\eta_0^2}{2} \mathbb{E} \left[\left\| \check{G}_0^t(\tilde{\mathbf{w}}^t) \right\|^2 \right]}_{\mathcal{E}_2} \\ &\quad - \underbrace{\eta_{m_k} \mathbb{E} \langle \nabla_{w_{m_k}} F_\lambda(\mathbf{w}^t), \check{G}_{m_k}^t(\tilde{\mathbf{w}}^t) \rangle}_{\mathcal{E}_3} + \underbrace{\frac{L\eta_{m_k}^2}{2} \mathbb{E} \left[\left\| \check{G}_{m_k}^t(\tilde{\mathbf{w}}^t) \right\|^2 \right]}_{\mathcal{E}_4} \end{aligned} \quad (26)$$

where in the second step we take expectation on both sides, first w.r.t. the random direction u , DP noise z , and the clipping event Q , then w.r.t the client m_k .

We bound \mathcal{E}_1 as the following:

$$\begin{aligned} &- \eta_0 \mathbb{E} \langle \nabla_{w_0} F_\lambda(\mathbf{w}^t), \check{G}_0^t(\tilde{\mathbf{w}}^t) \rangle \\ &= - \eta_0 \mathbb{E} \langle \nabla_{w_0} F_\lambda(\mathbf{w}^t), \check{G}_0^t(\tilde{\mathbf{w}}^t) - (1-P)\nabla_{w_0} F_\lambda(\tilde{\mathbf{w}}^t) + (1-P)\nabla_{w_0} F_\lambda(\tilde{\mathbf{w}}^t) \rangle \\ &= - \eta_0 \mathbb{E} \langle \nabla_{w_0} F_\lambda(\mathbf{w}^t), \check{G}_0^t(\tilde{\mathbf{w}}^t) - (1-P)\nabla_{w_0} F_\lambda(\tilde{\mathbf{w}}^t) \rangle \\ &- \eta_0 \mathbb{E} \langle \nabla_{w_0} F_\lambda(\mathbf{w}^t), (1-P)\nabla_{w_0} F_\lambda(\tilde{\mathbf{w}}^t) - (1-P)\nabla_{w_0} F_\lambda(\mathbf{w}^t) + (1-P)\nabla_{w_0} F_\lambda(\mathbf{w}^t) \rangle \end{aligned}$$

$$\begin{aligned}
&\stackrel{1)}{=} -(1-P)\eta_0\mathbb{E}\langle\nabla_{w_0}F_\lambda(\mathbf{w}^t),\nabla_{w_0}F_\lambda(\tilde{\mathbf{w}}^t)-\nabla_{w_0}F_\lambda(\mathbf{w}^t)\rangle \\
&\quad -\eta_0\mathbb{E}\langle\nabla_{w_0}F_\lambda(\mathbf{w}^t),(1-P)\nabla_{w_0}F_\lambda(\mathbf{w}^t)\rangle \\
&\stackrel{2)}{\leq}\frac{(1-P)\eta_0}{2}\mathbb{E}\left[\|\nabla_{w_0}F_\lambda(\mathbf{w}^t)\|^2\right]+\frac{(1-P)\eta_0}{2}\mathbb{E}\left[\|\nabla_{w_0}F_\lambda(\tilde{\mathbf{w}}^t)-\nabla_{w_0}F_\lambda(\mathbf{w}^t)\|^2\right]-(1-P)\eta_0\mathbb{E}\left[\|\nabla_{w_0}F_\lambda(\mathbf{w}^t)\|^2\right] \\
&\stackrel{3)}{\leq}-\frac{(1-P)\eta_0}{2}\mathbb{E}\left[\|\nabla_{w_0}F_\lambda(\mathbf{w}^t)\|^2\right]+\frac{\eta_0L}{2}\mathbb{E}\left[\|\tilde{\chi}^t-\chi^t\|^2\right] \tag{27}
\end{aligned}$$

where in 1) we use the fact that $\mathbb{E}\left[\check{G}_0^t(\tilde{\mathbf{w}}^t)-(1-P)\nabla_{x_0}F_\lambda(\tilde{\mathbf{w}}^t)\right]=0$, in 2) we applied the Cauchy–Schwarz inequality, and 3) follows by the smoothness of F_λ and the fact that $1-P\leq 1$

For \mathcal{E}_2 , we can further bound it based on Assumption A.2:

$$\begin{aligned}
&\frac{1}{2}\mathbb{E}\left[\|\check{G}_0^t(\tilde{\mathbf{w}}^t)\|^2\right] \\
&= \frac{1}{2}\mathbb{E}\left[\|\check{G}_0^t(\tilde{\mathbf{w}}^t)-(1-P)\nabla_{x_0}F_\lambda(\mathbf{w}^t)+(1-P)\nabla_{x_0}F_\lambda(\mathbf{w}^t)\|^2\right] \\
&\stackrel{1)}{\leq}\mathbb{E}\left[\|\check{G}_0^t(\tilde{\mathbf{w}}^t)-(1-P)\nabla_{x_0}F_\lambda(\mathbf{w}^t)\|^2\right]+(1-P)^2\mathbb{E}\left[\|\nabla_{x_0}F_\lambda(\mathbf{w}^t)\|^2\right] \\
&= \mathbb{E}\left[\|\check{G}_0^t(\tilde{\mathbf{w}}^t)-(1-P)\nabla_{x_0}F_\lambda(\tilde{\mathbf{w}}^t)+(1-P)\nabla_{x_0}F_\lambda(\tilde{\mathbf{w}}^t)-(1-P)\nabla_{x_0}F_\lambda(\mathbf{w}^t)\|^2\right] \\
&\quad + (1-P)^2\mathbb{E}\left[\|\nabla_{x_0}F_\lambda(\mathbf{w}^t)\|^2\right] \\
&\stackrel{2)}{\leq}2\mathbb{E}\left[\|\check{G}_0^t(\tilde{\mathbf{w}}^t)-(1-P)\nabla_{x_0}F_\lambda(\tilde{\mathbf{w}}^t)\|^2\right]+2(1-P)^2\mathbb{E}\left[\|\nabla_{x_0}F_\lambda(\tilde{\mathbf{w}}^t)-\nabla_{x_0}F_\lambda(\mathbf{w}^t)\|^2\right] \\
&\quad + (1-P)^2\mathbb{E}\left[\|\nabla_{x_0}F_\lambda(\mathbf{w}^t)\|^2\right] \\
&\stackrel{3)}{\leq}\frac{2(1-P)}{B}(2d_0\mathbb{E}\left[\|\nabla_{x_0}F(\mathbf{w}^t)\|^2\right]+2d_0\sigma_s^2+\frac{L^2}{2}\lambda^2d_0^3)+\frac{2P}{B}C^2d_0 \\
&\quad -\frac{2(1-P)^2}{B}\mathbb{E}\left[\|\nabla_{x_0}F_\lambda(\mathbf{w}^t)\|^2\right]+2\sigma_{dp}^2d_0+2(1-P)^2L^2\mathbb{E}\left[\|\tilde{\chi}^t-\chi^t\|^2\right]+(1-P)^2\mathbb{E}\left[\|\nabla_{x_0}F_\lambda(\mathbf{w}^t)\|^2\right] \\
&\stackrel{4)}{\leq}\frac{4(1-P)d_0}{B}\mathbb{E}\left[\|\nabla_{x_0}F(\mathbf{w}^t)\|^2\right]+(1-P)\mathbb{E}\left[\|\nabla_{x_0}F_\lambda(\mathbf{w}^t)\|^2\right]+2L^2\mathbb{E}\left[\|\tilde{\chi}^t-\chi^t\|^2\right]+\mathcal{G}_0 \tag{28}
\end{aligned}$$

where in 1) and 2) we applied the Cauchy–Schwarz inequality, and in 3) we substitute (21) in and use the L -smoothness of F_λ , and in (iv) we use the fact that $1-P\leq 1$ and let

$$\mathcal{G}_0 = \frac{4}{B}d_0\sigma_s^2 + \frac{L^2}{B}\lambda^2d_0^3 + \frac{2P}{B}C^2d_0 + 2\sigma_{dp}^2d_0$$

Similarly, For \mathcal{E}_3 :

$$-\eta_{m_k}\mathbb{E}\langle\nabla_{w_{m_k}}F_\lambda(\mathbf{w}^t),\check{G}_m^t(\tilde{\mathbf{w}}^t)\rangle \leq -\frac{(1-P)\eta_{m_k}}{2}\mathbb{E}\left[\|\nabla_{w_{m_k}}F_\lambda(\mathbf{w}^t)\|^2\right] + \frac{\eta_{m_k}L}{2}\mathbb{E}\left[\|\tilde{\chi}^t-\chi^t\|^2\right] \tag{29}$$

And for \mathcal{E}_4 :

$$\frac{1}{2}\mathbb{E}\left[\|\check{G}_{m_k}^t(\tilde{\mathbf{w}}^t)\|^2\right] \leq \frac{4(1-P)d_m}{B}\mathbb{E}\left[\|\nabla_{w_{m_k}}F(\mathbf{w}^t)\|^2\right] + (1-P)\mathbb{E}\left[\|\nabla_{w_{m_k}}F_\lambda(\mathbf{w}^t)\|^2\right] \tag{30}$$

$$+ 2L^2\mathbb{E}\left[\|\tilde{\chi}^t-\chi^t\|^2\right] + \mathcal{G}_m \tag{31}$$

where we let

$$\mathcal{G}_m = \frac{4}{B}d_m\sigma_s^2 + \frac{L^2}{B}\lambda^2d_m^3 + \frac{2P}{B}C^2d_m + 2\sigma_{dp}^2d_m \tag{32}$$

Substituting (27), (28), (29), and (31) into (26), we have

$$\begin{aligned}
& \mathbb{E} [F(\mathbf{w}^{t+1}) - F(\mathbf{w}^t)] \\
& \leq \mathbb{E} [F_\lambda(\mathbf{w}^t)] - \frac{(1-P)\eta_0}{2} \mathbb{E} [\|\nabla_{w_0} F_\lambda(\mathbf{w}^t)\|^2] + \frac{\eta_0 L}{2} \mathbb{E} [\|\tilde{\chi}^t - \chi^t\|^2] \\
& + \frac{4(1-P)d_0 L \eta_0^2}{B} \mathbb{E} [\|\nabla_{w_0} F(\mathbf{w}^t)\|^2] + (1-P)L\eta_0^2 \mathbb{E} [\|\nabla_{w_0} F_\lambda(\mathbf{w}^t)\|^2] + 2L^3\eta_0^2 \mathbb{E} [\|\tilde{\chi}^t - \chi^t\|^2] + L\eta_0^2 \mathcal{G}_0 \\
& - \frac{(1-P)\eta_{m_k}}{2} \mathbb{E} [\|\nabla_{w_{m_k}} F_\lambda(\mathbf{w}^t)\|^2] + \frac{\eta_{m_k} L}{2} \mathbb{E} [\|\tilde{\chi}^t - \chi^t\|^2] \\
& + \frac{4(1-P)d_{m_k} L \eta_{m_k}^2}{B} \mathbb{E} [\|\nabla_{w_{m_k}} F(\mathbf{w}^t)\|^2] + (1-P)L\eta_{m_k}^2 \mathbb{E} [\|\nabla_{w_{m_k}} F_\lambda(\mathbf{w}^t)\|^2] \\
& + 2L^3\eta_{m_k}^2 \mathbb{E} [\|\tilde{\chi}^t - \chi^t\|^2] + L\eta_{m_k}^2 \mathcal{G}_m \\
& \leq \mathbb{E} [F_\lambda(\mathbf{w}^t)] - \eta_0(1-P) \left(\frac{1}{2} - \eta_0 L\right) \mathbb{E} [\|\nabla_{w_0} F_\lambda(\mathbf{w}^t)\|^2] + \eta_0 L \left(\frac{1}{2} + 2\eta_0 L^2\right) \mathbb{E} [\|\tilde{\chi}^t - \chi^t\|^2] \\
& + \eta_0^2 \frac{4(1-P)d_0 L}{B} \mathbb{E} [\|\nabla_{w_0} F(\mathbf{w}^t)\|^2] + \eta_0^2 L \mathcal{G}_0 \\
& - \sum_{m=1}^M q_m \eta_m (1-P) \left(\frac{1}{2} - \eta_m L\right) \mathbb{E} [\|\nabla_{w_m} F_\lambda(\mathbf{w}^t)\|^2] + \sum_{m=1}^M q_m \eta_m L \left(\frac{1}{2} + 2\eta_m L^2\right) \mathbb{E} [\|\tilde{\chi}^t - \chi^t\|^2] \\
& + \sum_{m=1}^M q_m \eta_m^2 \frac{4(1-P)d_m L}{B} \mathbb{E} [\|\nabla_{w_m} F(\mathbf{w}^t)\|^2] + \sum_{m=1}^M q_m \eta_m^2 L \mathcal{G}_m \tag{33}
\end{aligned}$$

where in the last inequality we further take expectation w.r.t. client M and combine similar terms.

From (33), we utilize the properties of the smooth function (14) and (17) to turn all the smooth function F_λ into the true loss function F :

$$\begin{aligned}
& \mathbb{E} [F(\mathbf{w}^{t+1}) - F(\mathbf{w}^t)] \stackrel{1)}{\leq} \mathbb{E} [F_\lambda(\mathbf{w}^{t+1}) - F_\lambda(\mathbf{w}^t)] + L\lambda^2 d \\
& \stackrel{2)}{\leq} -\eta_0(1-P) \left(\frac{1}{2} - \eta_0 L\right) \left(\frac{1}{2} \mathbb{E} [\|\nabla_{x_0} F(\mathbf{w}^t)\|^2] - \frac{L^2}{4} \lambda^2 d_0^3\right) + \eta_0 L \left(\frac{1}{2} + 2\eta_0 L^2\right) \mathbb{E} [\|\tilde{\chi}^t - \chi^t\|^2] \\
& + \eta_0^2 \frac{4(1-P)d_0 L}{B} \mathbb{E} [\|\nabla_{x_0} F(\mathbf{w}^t)\|^2] + \eta_0^2 L \mathcal{G}_0 \\
& - \sum_{m=1}^M q_m \eta_m (1-P) \left(\frac{1}{2} - \eta_m L\right) \left(\frac{1}{2} \mathbb{E} [\|\nabla_{w_m} F(\mathbf{w}^t)\|^2] - \frac{L^2}{4} \lambda^2 d_m^3\right) \\
& + \sum_{m=1}^M q_m \eta_m L \left(\frac{1}{2} + 2\eta_m L^2\right) \mathbb{E} [\|\tilde{\chi}^t - \chi^t\|^2] \\
& + \sum_{m=1}^M q_m \eta_m^2 \frac{4(1-P)d_m L}{B} \mathbb{E} [\|\nabla_{w_m} F(\mathbf{w}^t)\|^2] + \sum_{m=1}^M q_m \eta_m^2 L \mathcal{G}_m + L\lambda^2 d \\
& \stackrel{3)}{\leq} -\sum_{m=0}^M q_m \eta_m (1-P) \left(\frac{1}{4} - \frac{\eta_m L(B + 8d_m)}{2B}\right) \mathbb{E} [\|\nabla_{w_m} F(\mathbf{w}^t)\|^2] \\
& + \sum_{m=0}^M q_m \eta_m L \left(\frac{1}{2} + 2\eta_m L^2\right) \mathbb{E} [\|\tilde{\chi}^t - \chi^t\|^2] + \sum_{m=0}^M q_m \eta_m \left(\frac{1}{2} - \eta_m L\right) \frac{L^2}{4} \lambda^2 d_m^3 \\
& + \sum_{m=0}^M q_m \eta_m^2 L \mathcal{G}_m + L\lambda^2 d \\
& \stackrel{4)}{\leq} -\sum_{m=0}^M q_m \eta_m (1-P) \left(\frac{1}{4} - \frac{\eta_m L(B + 8d_m)}{2B}\right) \mathbb{E} [\|\nabla_{w_m} F(\mathbf{w}^t)\|^2]
\end{aligned}$$

$$\begin{aligned}
& + \sum_{m=0}^M q_m \eta_m L \left(\frac{1}{2} + 2\eta_m L^2 \right) \mathbb{E} \left[\|\tilde{\chi}^t - \chi^t\|^2 \right] \\
& + \sum_{m=0}^M q_m \eta_m \frac{L^2}{8} \lambda^2 d_m^3 + \sum_{m=0}^M q_m \eta_m^2 L \left(\frac{4}{B} d_m \sigma_s^2 + \frac{(4-B)L^2}{4B} \lambda^2 d_m^3 + \frac{2P}{B} C^2 d_m + 2\sigma_{dp}^2 d_m \right) + L\lambda^2 d \\
& \stackrel{5)}{\leq} - \sum_{m=0}^M q_m \eta_m (1-P) \left(\frac{1}{4} - \frac{\eta_m L(B+8d_m)}{2B} \right) \mathbb{E} \left[\|\nabla_{w_m} F(\mathbf{w}^t)\|^2 \right] \\
& + \sum_{m=0}^M q_m \eta_m L \left(\frac{1}{2} + 2\eta_m L^2 \right) \mathbb{E} \left[\|\tilde{\chi}^t - \chi^t\|^2 \right] + \mathcal{A}_1 \tag{34}
\end{aligned}$$

where 1) and 2) follows from equation (14) and (17) in Theorem A.6 respectively. In 3), we let $q_0 = 1$ and combine similar terms. In 4), we substitute in (32). Lastly, in 5), we denote

$$\mathcal{A}_1 = \sum_{m=0}^M q_m \eta_m \frac{L^2}{8} \lambda^2 d_m^3 + \sum_{m=0}^M q_m \eta_m^2 L \left(\frac{4}{B} d_m \sigma_s^2 + \frac{(4-B)L^2}{4B} \lambda^2 d_m^3 + \frac{2P}{B} C^2 d_m + 2\sigma_{dp}^2 d_m \right) + L\lambda^2 d \tag{35}$$

for the convenience of notation.

We thus complete the proof. \square

Now, recall the definition of the Lyapunov function V^t :

$$V^t = F(\mathbf{w}^t) + \sum_{i=1}^{\tau} \gamma_i \|\chi^{t+1-i} - \chi^{t-i}\|^2$$

We utilize the Lyapunov function to prove the following lemma for eliminating model delay.

Lemma D.2. *Under Theorem A.1-A.4, and assume the client delay τ_m is uniformly upper bounded by τ , we have the following lemma:*

$$\mathbb{E} [V^{t+1} - V^t] \leq -\frac{1-P}{8} \min\{q_m \eta_m\} \mathbb{E} \left[\|\nabla_{\mathbf{w}} F(\mathbf{w}^t)\|^2 \right] + \mathcal{A}_1 + \mathcal{A}_2$$

Proof. Before we give the proof of Theorem D.2, we first provide some useful facts that reveal properties of the delayed parameters.

Recall that $\tilde{\chi}^t$ denote the delayed parameters on all clients, and χ^t denote the non-delayed version. Let $\mathcal{F}_1 = \mathbb{E} \left[\|\chi^{t+1} - \chi^t\|^2 \right]$, $\mathcal{F}_2 = \mathbb{E} \left[\|\tilde{\chi}^t - \chi^t\|^2 \right]$.

For \mathcal{F}_1 :

$$\begin{aligned}
& \mathbb{E} \left[\|\chi^{t+1} - \chi^t\|^2 \right] \\
& = \eta_m^2 \mathbb{E} \left[\left\| \check{G}_{m_k}^t(\tilde{\mathbf{w}}^t) \right\|^2 \right] \\
& \leq \sum_{m=1}^M q_m \eta_m^2 \frac{2(1-P)d_m}{B} \mathbb{E} \left[\left\| \nabla_{w_{m_k}} F(\mathbf{w}^t) \right\|^2 \right] + \sum_{m=1}^M q_m \eta_m^2 \frac{(1-P)}{2} \mathbb{E} \left[\left\| \nabla_{w_{m_k}} F_\lambda(\mathbf{w}^t) \right\|^2 \right] \\
& + \sum_{m=1}^M q_m \eta_m^2 \left(L^2 \mathbb{E} \left[\|\tilde{\chi}^t - \chi^t\|^2 \right] + \frac{1}{2} \mathcal{G}_m \right) \\
& \leq \sum_{m=1}^M q_m \eta_m^2 \frac{2(1-P)d_m}{B} \mathbb{E} \left[\left\| \nabla_{w_{m_k}} F(\mathbf{w}^t) \right\|^2 \right] + \sum_{m=1}^M q_m \eta_m^2 \frac{(1-P)}{2} \left(2\mathbb{E} \left[\left\| \nabla_{w_{m_k}} F(\mathbf{w}^t) \right\|^2 \right] + \frac{L^2}{2} \lambda^2 d_m^3 \right) \\
& + \sum_{m=1}^M q_m \eta_m^2 \left(L^2 \mathbb{E} \left[\|\tilde{\chi}^t - \chi^t\|^2 \right] + \frac{1}{2} \mathcal{G}_m \right)
\end{aligned}$$

$$= \sum_{m=1}^M q_m \eta_m^2 \frac{(1-P)(2d_m+B)}{B} \mathbb{E} \left[\left\| \nabla_{w_{m_k}} F(\mathbf{w}^t) \right\|^2 \right] + \sum_{m=1}^M q_m \eta_m^2 \left(\frac{L^2}{4} \lambda^2 d_m^3 + L^2 \mathbb{E} \left[\|\tilde{\chi}^t - \chi^t\|^2 \right] + \frac{1}{2} \mathcal{G}_m \right) \quad (36)$$

For \mathcal{F}_2 , under uniformly bounded delay, we have

$$\begin{aligned} & \mathbb{E} \left[\|\tilde{\chi}^t - \chi^t\|^2 \right] \\ & \leq \mathbb{E} \left[\left\| \sum_{i=1}^{\tau} (\chi^{i+1} - \chi^i) \right\|^2 \right] \\ & \leq \tau \sum_{i=1}^{\tau} \mathbb{E} \left[\|\chi^{i+1} - \chi^i\|^2 \right] \end{aligned} \quad (37)$$

where the last inequality follows by Cauchy-Schwarz Inequality. By the definition of V^t :

$$\begin{aligned} & \mathbb{E} [V^{t+1} - V^t] \\ & = \mathbb{E} \left[F(\mathbf{w}^{t+1}) + \sum_{i=1}^{\tau} \gamma_i \|\chi^{t+2-i} - \chi^{t+1-i}\|^2 \right] - \mathbb{E} \left[F(\mathbf{w}^t) + \sum_{i=1}^{\tau} \gamma_i \|\chi^{t+1-i} - \chi^{t-i}\|^2 \right] \\ & = \mathbb{E} [F(\mathbf{w}^{t+1}) - F(\mathbf{w}^t)] + \sum_{i=1}^{\tau} \gamma_i \mathbb{E} \left[\|\chi^{t+2-i} - \chi^{t+1-i}\|^2 \right] - \sum_{i=1}^{\tau} \gamma_i \mathbb{E} \left[\|\chi^{t+1-i} - \chi^{t-i}\|^2 \right] \\ & \stackrel{1)}{\leq} - \sum_{m=0}^M q_m \eta_m (1-P) \left(\frac{1}{4} - \frac{\eta_m L(B+8d_m)}{2B} \right) \mathbb{E} \left[\|\nabla_{w_m} F(\mathbf{w}^t)\|^2 \right] \\ & \quad + \sum_{m=0}^M q_m \eta_m L \left(\frac{1}{2} + 2\eta_m L^2 \right) \mathbb{E} \left[\|\tilde{\chi}^t - \chi^t\|^2 \right] + \mathcal{A}_1 \\ & \quad + \underbrace{\gamma_1 \mathbb{E} \left[\|\chi^{t+1} - \chi^t\|^2 \right]}_{\mathcal{F}_1} + \sum_{i=1}^{\tau-1} (\gamma_{i+1} - \gamma_i) \mathbb{E} \left[\|\chi^{t+1-i} - \chi^{t-i}\|^2 \right] - \gamma_{\tau} \mathbb{E} \left[\|\chi^{t+1-\tau} - \chi^{t-\tau}\|^2 \right] \\ & \stackrel{2)}{\leq} - \sum_{m=0}^M q_m \eta_m (1-P) \left(\frac{1}{4} - \frac{\eta_m L(B+8d_m)}{2B} \right) \mathbb{E} \left[\|\nabla_{w_m} F(\mathbf{w}^t)\|^2 \right] \\ & \quad + \sum_{m=0}^M q_m \eta_m L \left(\frac{1}{2} + 2\eta_m L^2 \right) \mathbb{E} \left[\|\tilde{\chi}^t - \chi^t\|^2 \right] + \mathcal{A}_1 \\ & \quad + \sum_{m=1}^M q_m \eta_m^2 \gamma_1 \frac{(1-P)(2d_m+B)}{B} \mathbb{E} \left[\left\| \nabla_{w_{m_k}} F(\mathbf{w}^t) \right\|^2 \right] + \sum_{m=1}^M q_m \eta_m^2 \gamma_1 \left(\frac{L^2}{4} \lambda^2 d_m^3 + L^2 \mathbb{E} \left[\|\tilde{\chi}^t - \chi^t\|^2 \right] + \frac{1}{2} \mathcal{G}_m \right) \\ & \quad + \sum_{i=1}^{\tau-1} (\gamma_{i+1} - \gamma_i) \mathbb{E} \left[\|\chi^{t+1-i} - \chi^{t-i}\|^2 \right] - \gamma_{\tau} \mathbb{E} \left[\|\chi^{t+1-\tau} - \chi^{t-\tau}\|^2 \right] \\ & \stackrel{3)}{=} - \eta_0 (1-P) \left(\frac{1}{4} - \frac{\eta_0 L(B+8d_0)}{2B} \right) \mathbb{E} \left[\|\nabla_{x_0} F(\mathbf{w}^t)\|^2 \right] \\ & \quad - \sum_{m=1}^M q_m \eta_m (1-P) \left(\frac{1}{4} - \frac{\eta_m L(B+8d_m)}{2B} - \frac{\eta_m \gamma_1 (2d_m+B)}{B} \right) \mathbb{E} \left[\|\nabla_{w_m} F(\mathbf{w}^t)\|^2 \right] \\ & \quad + \left\{ \eta_0 L \left(\frac{1}{2} + 2\eta_0 L^2 \right) + \sum_{m=1}^M q_m \eta_m L \left(\frac{1}{2} + 2\eta_m L^2 + \eta_m \gamma_1 L \right) \right\} \underbrace{\mathbb{E} \left[\|\tilde{\chi}^t - \chi^t\|^2 \right]}_{\mathcal{F}_2} \\ & \quad + \mathcal{A}_1 + \sum_{m=1}^M q_m \eta_m^2 \gamma_1 \left(\frac{L^2}{4} \lambda^2 d_m^3 + \frac{1}{2} \mathcal{G}_m \right) \end{aligned}$$

$$\begin{aligned}
& + \sum_{i=1}^{\tau-1} (\gamma_{i+1} - \gamma_i) \mathbb{E} \left[\|\chi^{t+1-i} - \chi^{t-i}\|^2 \right] - \gamma_\tau \mathbb{E} \left[\|\chi^{t+1-\tau} - \chi^{t-\tau}\|^2 \right] \\
& \stackrel{4)}{\leq} -\eta_0(1-P) \left(\frac{1}{4} - \frac{\eta_0 L(B+8d_0)}{2B} \right) \mathbb{E} \left[\|\nabla_{x_0} F(\mathbf{w}^t)\|^2 \right] \\
& - \sum_{m=1}^M q_m \eta_m (1-P) \left(\frac{1}{4} - \frac{\eta_m L(B+8d_m)}{2B} - \frac{\eta_m \gamma_1 (2d_m + B)}{B} \right) \mathbb{E} \left[\|\nabla_{w_m} F(\mathbf{w}^t)\|^2 \right] \\
& + \sum_{i=1}^{\tau-1} \left(\gamma_{i+1} - \gamma_i + \tau \left(\eta_0 L \left(\frac{1}{2} + 2\eta_0 L^2 \right) + \sum_{m=1}^M q_m \eta_m L \left(\frac{1}{2} + 2\eta_m L^2 + \eta_m \gamma_1 L \right) \right) \right) \mathbb{E} \left[\|\chi^{t+1-i} - \chi^{t-i}\|^2 \right] \\
& - \left(\gamma_\tau - \tau \left(\eta_0 L \left(\frac{1}{2} + 2\eta_0 L^2 \right) + \sum_{m=1}^M q_m \eta_m L \left(\frac{1}{2} + 2\eta_m L^2 + \eta_m \gamma_1 L \right) \right) \right) \mathbb{E} \left[\|\chi^{t+1-\tau} - \chi^{t-\tau}\|^2 \right] \\
& + \mathcal{A}_1 + \mathcal{A}_2. \tag{38}
\end{aligned}$$

Above, we used Theorem D.1 in step (1), substituted in (36) for \mathcal{F}_1 in step (2), substituted in (37) for \mathcal{F}_2 in step (3), and defined

$$\begin{aligned}
\mathcal{A}_2 & := \sum_{m=1}^M q_m \eta_m^2 \gamma_1 \left(\frac{L^2}{4} \lambda^2 d_m^3 + \frac{1}{2} \mathcal{G}_m \right) \\
& = \sum_{m=1}^M q_m \eta_m^2 \gamma_1 \left(\frac{L^2}{4} \lambda^2 d_m^3 + \frac{2}{B} d_m \sigma_s^2 + \frac{L^2}{2B} \lambda^2 d_m^3 + \frac{P}{B} C^2 d_m + \sigma_{dp}^2 d_m \right). \tag{39}
\end{aligned}$$

From (38), we choose the following relationship for $\gamma_1, \gamma_2, \dots, \gamma_m$:

$$\gamma_1 = \frac{\tau^2 \left(\eta_0 L \left(\frac{1}{2} + 2\eta_0 L^2 \right) + \sum_{m=1}^M q_m \eta_m L \left(\frac{1}{2} + 2\eta_m L^2 \right) \right)}{1 - \tau^2 \sum_{m=1}^M q_m \eta_m^2 L^2} \tag{40}$$

$$\gamma_{i+1} = \gamma_i - \tau \left(\eta_0 L \left(\frac{1}{2} + 2\eta_0 L^2 \right) + \sum_{m=1}^M q_m \eta_m L \left(\frac{1}{2} + 2\eta_m L^2 + \eta_m \gamma_1 L \right) \right)$$

and we can verify that

$$\gamma_\tau - \tau \left(\eta_0 L \left(\frac{1}{2} + 2\eta_0 L^2 \right) + \sum_{m=1}^M q_m \eta_m L \left(\frac{1}{2} + 2\eta_m L^2 + \eta_m \gamma_1 L \right) \right) \geq 0$$

We further let

$$\eta_0 \leq \frac{B}{4L(B+8d_0)}, \eta_m \leq \frac{B}{4L(B+8d_0) + 8\gamma_1(2d_m + B)},$$

and we finally have

$$\begin{aligned}
\mathbb{E} [V^{t+1} - V^t] & \leq -\frac{\eta_0}{8} (1-P) \mathbb{E} \left[\|\nabla_{x_0} F(\mathbf{w}^t)\|^2 \right] - \sum_{m=1}^M \frac{q_m \eta_m}{8} (1-P) \mathbb{E} \left[\|\nabla_{w_m} F(\mathbf{w}^t)\|^2 \right] + \mathcal{A}_1 + \mathcal{A}_2 \\
& \leq -\frac{1-P}{8} \min_m q_m \eta_m \mathbb{E} \left[\|\nabla_{\mathbf{w}} F(\mathbf{w}^t)\|^2 \right] + \mathcal{A}_1 + \mathcal{A}_2 \tag{41}
\end{aligned}$$

which completes the proof. \square

E Discussion of Differential Privacy under Various Settings

Overview of DPZV's Privacy Mechanisms. DPZV protects privacy through two main mechanisms: 1) *Zeroth-Order (ZO) Optimization*. By eliminating the need to transmit backward gradients, DPZV mitigates conventional gradient-based leakage [16]. Specifically, no unperturbed gradients are ever exchanged among participants. 2) *Controllable Differential Privacy (DP)*. Each participant interacts only through black-box queries and responses augmented with DP-based noise. This randomized protocol further shields sensitive information from reconstruction or inference attacks.

E.1 Protection Against an Honest-but-Curious Threat Model

In an *honest-but-curious* scenario, adversaries seek private insights (labels or features) without deviating from the protocol. Two common types of attacks are:

Label Inference Attacks. Such attacks typically exploit exact gradient signs or rely on known model architectures to backtrack label information [13, 21]. Under DPZV, *unbiased gradients are never shared*, and the server model remains inaccessible to other participants. Clients observe only *stochastic ZO outputs* with added noise, preventing them from reverse-engineering labels via gradient signals.

Feature Inference Attacks. Adversaries may attempt feature or data reconstruction [16] by leveraging gradient disclosures or conducting model inversion. DPZV thwarts such efforts by disallowing adaptive queries on the client’s internal parameters; only scalar function evaluations flow to and from the server. Additionally, the injected DP noise obscures potential patterns that attackers might exploit for reconstructing sensitive features.

Moreover, both label and feature inference methods often assume knowledge of the dataset domain or direct model access, which is not given in DPZV’s design. Task details (e.g., label distributions, model layers) are held privately by each party, limiting the adversary’s capacity to launch sophisticated inversion or inference attacks.

E.2 Protection Against Post-Training Attacks

Post-training adversaries typically aim to infer sensitive data from a *final, trained model* [2]. Since DPZV applies differential privacy *throughout* training, the final model parameters satisfy rigorous (ϵ, δ) -DP guarantees. Hence, even if the trained model is released or accessed, the level of noise injected ensures that the adversary cannot reliably distinguish any single individual’s data—reducing vulnerability to membership inference or model-inversion attacks [18]. This formal DP framework remains robust regardless of downstream usage or queries on the finalized model.

In summary, by combining ZO optimization with DP noise injection, DPZV provides comprehensive protection against both *honest-but-curious* and *post-training* adversaries across diverse privacy threat scenarios.

F Memory Cost

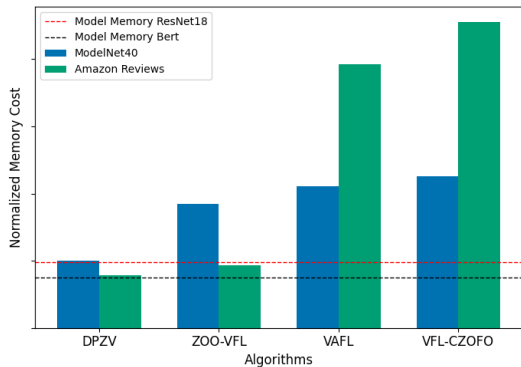


Figure 6: Normalized memory cost in training for each method. DPZV requires the smallest memory allocation in both datasets, almost the same as model memory itself. This shows the memory efficiency of DPZV, allowing superior performance on large-scale neural networks.

Figure 6 compares the GPU memory consumption, with memory values normalized for readability. We compare the memory cost on larger models, where we use ResNet for image classification and BERT for sequence classification. We record the highest memory peak to show the total

required memory for each method on training large models. We observe that DPZV requires memory approximately equal to the model size, whereas the first-order method VAFL demands more than twice the model size. Compared to ZOO-VFL, DPZV achieves further memory savings by leveraging MeZO. *These results highlight the scalability of DPZV, making it well-suited for deploying large pretrained language models in VFL scenarios.*

G Choice of all Hyperparameters

In this section, we show all the chosen Hyperparameters, including learning rate for the four datasets and ZO and DP parameters in Sec. 7:

Table 2: All learning rate choices

DATASET		VAFL	ZOO-VFL	VFL-CZOFO	DPZV (OURS)
MNIST	η_0	0.005	0.005	0.005	0.005
	η_m	0.001	5×10^{-5}	1×10^{-7}	5×10^{-4}
CIFAR-10	η_0	0.005	0.005	0.005	0.005
	η_m	0.001	5×10^{-5}	5×10^{-8}	1×10^{-4}
MODELNET40	η_0	1×10^{-4}	1×10^{-5}	5×10^{-7}	1×10^{-5}
	η_m	1×10^{-5}	1×10^{-5}	5×10^{-7}	1×10^{-5}
AMAZON REVIEW	η_0	1×10^{-5}	5×10^{-7}	1×10^{-6}	5×10^{-7}
	η_m	1×10^{-5}	5×10^{-7}	1×10^{-6}	5×10^{-7}

Table 3: Other Hyperparameters

PARAMETER	VALUE	EXPLANATION
C	10	<i>DP clipping threshold</i>
λ	0.001	<i>Scale of perturbation for ZOO</i>
m	0.9	<i>Momentum parameter</i>
δ	1×10^{-5}	<i>DP error level</i>
n	5	<i>Number of perturbation for VFL-CZOFO</i>